



Original article

Dibasic biphenyl H₃ receptor antagonists: Steric tolerance for a lipophilic side chain

Fabrizio Bordi^a, Silvia Rivara^{a,*}, Elisa Dallaturca^a, Caterina Carmi^a, Daniele Pala^a, Alessio Lodola^a, Federica Vacondio^a, Lisa Flammini^b, Simona Bertoni^b, Vigilio Ballabeni^b, Elisabetta Barocelli^b, Marco Mor^a

^a Dipartimento Farmaceutico, Università degli Studi di Parma, V.le G.P. Usberti 27/A, I-43124 Parma, Italy

^b Dipartimento di Scienze Farmacologiche, Biologiche e Chimiche Applicate, Università degli Studi di Parma, V.le G.P. Usberti 27/A, I-43124 Parma, Italy

ARTICLE INFO

Article history:

Received 5 August 2011

Received in revised form

7 November 2011

Accepted 10 December 2011

Available online 20 December 2011

Keywords:

Histamine H₃ receptor

H₃-antagonist

NMR analysis

ABSTRACT

Within a series of histamine H₃-antagonists characterized by a biphenyl core and two basic groups, we identified (S)-1-[[4'-((2-methylpyrrolidin-1-yl)methyl)biphenyl-4-yl]methyl]piperidine as a lead scaffold to introduce an additional lipophilic chain at the benzylic carbon close to the pyrrolidine ring. A series of derivatives was synthesized and tested for their binding affinity at human and rat histamine H₃ receptors, and for their antagonist potency. For compounds with two chiral centers, the synthetic procedure provided mixtures of diastereomeric couples, which were separated by flash chromatography. Combination of experimental NMR data and molecular dynamics simulation allowed the assignment of absolute stereochemistry, based on characteristic differences detected within each diastereomeric couple. The additional lipophilic group was tolerated by the receptor, supporting the hypothesis that the two regions described within the H₃ receptor binding site can be simultaneously occupied by antagonists. Diastereoisomers with opposite chirality at the benzylic carbon showed limited or no stereoselectivity at both human and rat receptors.

© 2011 Elsevier Masson SAS. All rights reserved.

1. Introduction

The histaminergic system is involved in the regulation of several physiological processes. The natural ligand histamine is produced from the amino acid L-histidine and exerts its actions through the activation of four distinct G-protein-coupled receptors (GPCRs), known as H₁, H₂, H₃ and H₄ [1]. While antagonists of the H₁ receptor are widely used in the treatment of allergic responses [2], H₂ receptor antagonists inhibit gastric acid secretion, finding application in the treatment of peptic ulcer and gastroesophageal reflux disease [3]. H₄-antagonists have immunomodulatory actions and are under investigation as anti-inflammatory and anti-allergic drugs [4].

Identified in 1983 by Arrang and co-workers [5], the histamine H₃ receptors are primarily located in the central nervous system (CNS). They have a predominantly presynaptic localization and they modulate, through a negative feed-back mechanism, the biosynthesis and release of histamine [6]. In addition, H₃ receptors act as heteroreceptors, inhibiting the release of different

neurotransmitters, including norepinephrine [7,8], dopamine [9], serotonin [10], GABA [11], glutamate [12] and acetylcholine [13]. It has been observed that administration of H₃-antagonists in the CNS induces increased availability of these neurotransmitters, causing improvement in cognition and attention in animal models [14,15]. Thus, H₃-antagonists have been proposed in the treatment of cognitive disorders, such as attention deficit hyperactivity disorder (ADHD), Parkinson's and Alzheimer's diseases, as well as of narcolepsy, obesity, dementia, schizophrenia and epilepsy, and a number of compounds are currently evaluated in clinical trials [16–20].

First generation H₃-antagonists were characterized by an imidazole ring, in analogy with the natural ligand histamine [16,21,22]. However, imidazole-based antagonists showed possible drawbacks, such as affinity for CYP450, causing potential drug–drug interactions, poor brain penetration, due to the presence of polar hydrogen-bonding groups, and significant data discrepancies across species [23,24]. Thus, to overcome these drawbacks, many research efforts have been focused on the discovery and development of non-imidazole H₃-antagonists. Despite significant differences in compounds molecular weight and polarity, a general pharmacophore model has been developed for non-imidazole H₃-

* Corresponding author. Tel.: +39 0521 905062; fax: +39 0521 905006.
E-mail address: silvia.rivara@unipr.it (S. Rivara).

antagonists. They are usually characterized by a basic group, often a tertiary cyclic amine, connected through an aliphatic spacer to a second pharmacophoric fragment which includes, depending on the particular series, a lipophilic substituent (e.g. **1** and **2**, Fig. 1), a second basic portion (e.g. **3** and **4**, Fig. 1), or a hydrophilic substituent (e.g. **5**, Fig. 1) [18,24,25].

We have recently described a series of non-imidazole H₃-antagonists characterized by a central biphenyl scaffold connected, via alkyl spacers, to two basic groups [26,27]. This series was the result of a structural rigidification, obtained replacing the flexible polymethylene linker of a previous series with the rigid biphenyl scaffold [28,29]. The most potent derivative (**6**, Fig. 1) showed subnanomolar affinity for human and rat H₃ receptors (hH₃ pK_i = 9.47, rH₃ pK_i = 8.92). When docked within a model of rat H₃ receptor, two possible accommodations were identified for **6**. In the “horizontal” arrangement, compound **6** is perpendicular to the helix bundle and the piperidine nitrogens interact with Asp114 in transmembrane helix (TM) 3 and Glu206 in TM5. These amino acids are supposed to interact with the basic nitrogen and the imidazole ring of histamine, respectively, on the basis of mutagenesis studies. In the “vertical” arrangement, compound **6** lies parallel to the transmembrane helices and its basic centers interact with Asp114 and with Asn404 in TM7, located at the end of a second pocket perpendicular to that supposed to host the natural agonist [26]. Indeed, other docking studies on homology-based models of the H₃ receptor provided either “horizontal” or “vertical” poses for H₃-antagonists [30–34]. The possibility that two perpendicular pockets could simultaneously exist into the H₃ receptor implies that dibasic H₃-antagonists with a perpendicular side chain could undertake favorable interactions with the receptor binding site. This hypothesis is supported by some examples of dibasic H₃-antagonists with a lipophilic side chain, recently reported in literature (Fig. 2) [35–37].

Therefore, to explore and further extend the structure-activity relationships (SARs) on our class of biphenyl-based H₃-antagonists, new derivatives carrying a lipophilic side chain were prepared. In these compounds (**7–24**, Table 1) the biphenyl core is linked to two basic groups (R¹ and R²) through methylene spacers, and the additional side chain (R³) is attached to a methylene linker. The tolerance of the H₃ receptor to the steric hindrance of the R³ substituent was first evaluated, with substituents of different size and shape (**9–12**, Table 1). Then, the best tolerated *n*-butyl R³ group was maintained, and the effect of 2-methylpiperidine or 2-methylpyrrolidine as R² substituent was investigated (**12–18**, Table 1). Finally, the R² group providing the best affinity values, i.e. an (*S*)-2-methylpyrrolidine, was maintained and the lipophilic R³ substituent was replaced by bulkier groups (**19–24**, Table 1).

When the additional side chain was inserted close to a chiral 2-methylpyrrolidine or 2-methylpiperidine (**13–24**, Table 1), the

synthetic protocol led to couples of diastereomeric compounds, which were separated and singularly tested, to evaluate possible stereoselectivity. These couples resulted composed by two isomers with characteristic differences in their NMR spectra, also shown by their intermediates lacking the R¹ piperidine ring. To study the relationship between conformational equilibria and compound stereochemistry, we performed molecular dynamics simulations for the intermediates **29c,d** (Scheme 2), comparing calculated and experimental NMR data. As simulations for these two stereoisomers were in good agreement with their spectra, the characteristic differences observed within each diastereomeric couple were applied to the assignment of absolute stereochemistry.

2. Chemistry

Compounds **7–8** were synthesized starting from commercially available 4,4'-bis(chloromethyl)-biphenyl **25**, as reported in Scheme 1. Monosubstitution of **25** with piperidine to the intermediate **26**, followed by reaction with optically pure pyrrolidines, led to the desired products (Scheme 1). The synthetic route to compounds **9–24** and **34–35** is described in Scheme 2. Derivatives **9–11** were obtained from 4-iodobenzaldehyde **27**, that was reacted with benzyl zinc bromide and appropriate amine to obtain the iodophenyl intermediates **28a–b**. These compounds were submitted to Suzuki coupling giving the corresponding biphenyl derivatives **29a–b**. Finally, mesylation of **29a–b** followed by substitution with the appropriate amine gave the final compounds **9–11**. Reaction of **27** with butyl magnesium bromide led to the secondary alcohol **30**, that was coupled with 4-hydroxymethylphenylboronic acid to **31** and substituted with piperidine to obtain the final product **12**. Compounds **13–18** and **34** were synthesized from alcohol **30**, that was first oxidized to ketone **32a**, then reacted with the proper amine and reduced to give **28c–h** and **28p**. As already described, these iodophenyl intermediates were submitted to Suzuki coupling (to intermediates **29c–h**), followed by mesylation and amine substitution, to obtain products **13–18**. Compound **35** was obtained from **28p** by Suzuki coupling reaction. Similar procedures were employed to synthesize compounds **19–20** and **21–24**. Compounds **19** and **20** were obtained from 4-iodobenzonitrile **33**, that was reacted with 3-methoxypropyl magnesium chloride followed by hydrolysis to **32b**. Ketone **32b** was converted to **28i–j** by reductive amination with (*S*)-2-methylpyrrolidine. Suzuki coupling of **28i–j** (to **29i–j**), followed by mesylation and substitution with piperidine, gave the target compounds **19–20**. Final products **21–24** were prepared from **27** and allyloxybenzene derivatives to obtain ketones **32c–d**, that were reductively aminated with (*S*)-2-methylpyrrolidine to **28k–n**. Suzuki coupling of **28k–n** and substitution allowed to obtain products **21–24**. Finally, compound **34** was obtained following the same synthetic route (i.e. Suzuki

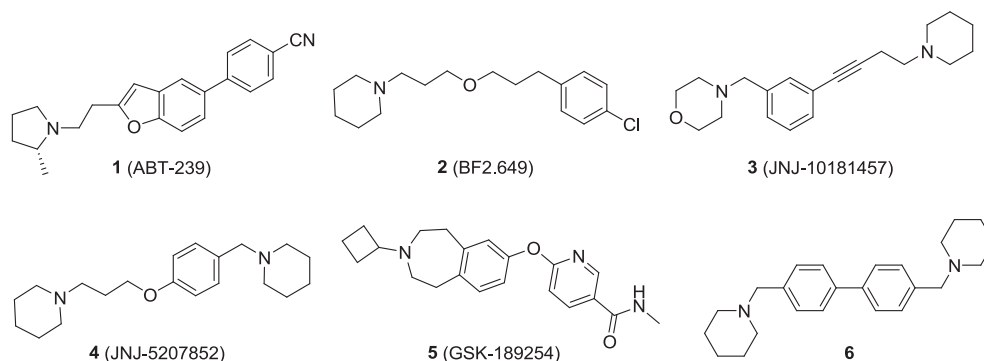


Fig. 1. Representative non-imidazole H₃-antagonists.

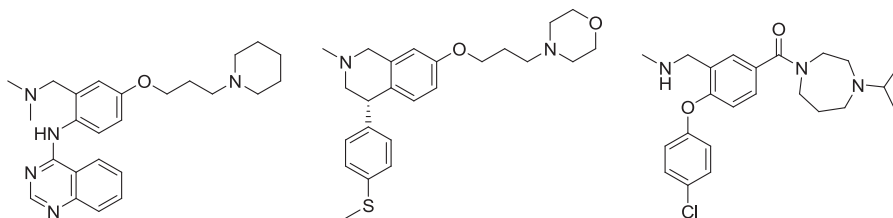


Fig. 2. Dibasic H₃-antagonists carrying a lipophilic substituent.

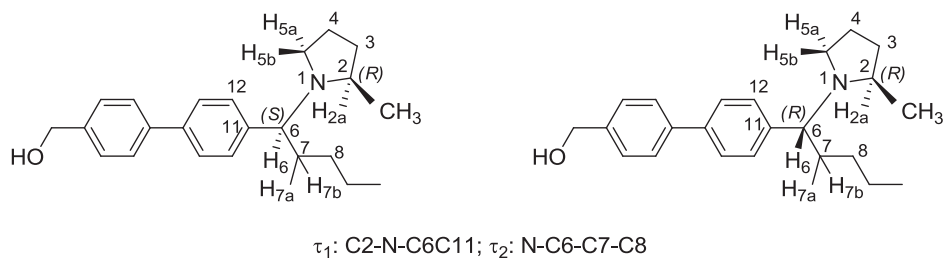


Fig. 3. Diastereoisomers **29c** and **29d** with atom numbering used for NMR and molecular modeling discussion, and τ_1 and τ_2 dihedral angle definition. The notation “a” or “b” refers to the relative position of protons with respect to the pyrrolidine plane: protons “a” are below the ring plane, while protons “b” are above the plane.

coupling and substitution with amine) from commercially available iodophenyl derivative **28o**.

3. Pharmacology

Histamine H₃ receptor affinity of the newly synthesized compounds was measured by displacement of [³H]-(*R*)- α -methyl-histamine ([³H]RAMHA) from GPCR97-transfected SK-N-MC cells stably expressing the human H₃ receptor [38], and from rat cerebral

cortex membranes [39]. H₃ Receptor antagonist potency was evaluated on SK-N-MC cells expressing the human H₃ receptor and the reporter gene β -galactosidase, by a colorimetric assay [40].

Histamine H₄ receptor affinity of the new molecules was measured by displacement of [³H]-histamine from GPCR97-transfected SK-N-MC cells stably expressing the human H₄ receptor [38].

In terms of selectivity, the compounds under study were investigated in the functional assays performed on guinea-pig

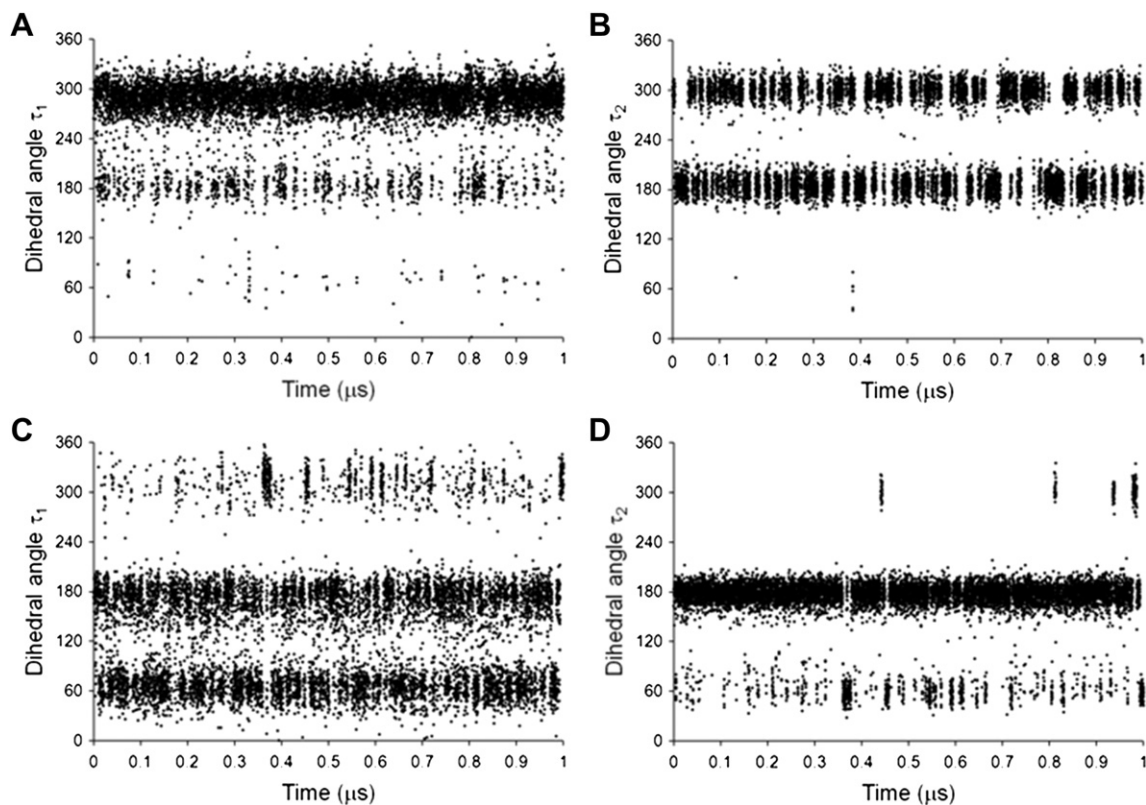


Fig. 4. Time evolution of dihedral angles τ_1 (C2-N1-C6-C11, panels A and C) and τ_2 (N1-C6-C7-C8, panels B and D) for (*R,S*) isomer (panels A, B) and (*R,R*) isomer (panels C, D).

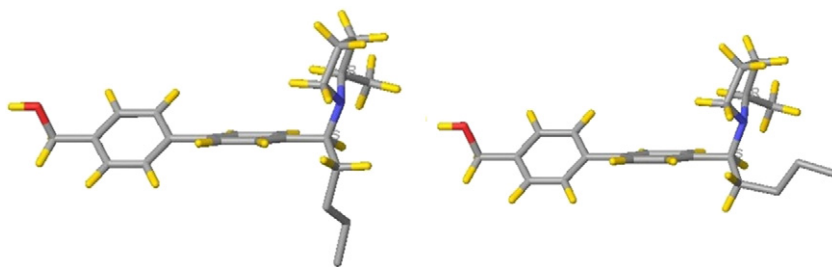


Fig. 5. Representative conformations of the (*S,R*) isomer with $\tau_1 \approx 300^\circ$ and $\tau_2 \approx 180^\circ$ (left), or $\tau_2 \approx 300^\circ$ (right).

isolated ileum (histamine H_1 receptor) and atria (histamine H_2 receptor) pharmacologically stimulated [41].

4. Results and discussion

4.1. Structure–activity relationships

Binding affinity and antagonist potency data for the newly synthesized compounds are reported in Table 1, together with those for the reference compound **6**. Replacement of one piperidine of the lead compound **6** with a 2-methylpyrrolidine provided better binding affinities when the methyl substituent was in (*S*) configuration (**8**). (*R*)-Methylpyrrolidine (**7**) was tolerated by human and rat receptors, but led to a slight reduction of binding affinity compared to the piperidine ring. Compound **8** showed subnanomolar binding affinity at both human and rat H_3 receptors, and remarkable antagonist potency at the human H_3 receptor. The higher binding affinity displayed by (*S*)-**8** was unexpected, as other series of H_3 -antagonists, having a terminal methylpyrrolidine group, had shown higher affinity for the (*R*) isomers [42,43].

The first results suggested that a benzyl substituent was detrimental for binding affinity, as can be seen from binding data of compounds **9** and **10**. The de-benzyl analog of **10**, previously synthesized by us, had shown hH_3 $pK_i = 8.66$ and rH_3 $pK_i = 8.88$ [27]. Similarly, compound **11**, tested as a mixture of diastereoisomers, showed lower binding affinity than **7**, both carrying a (*R*)-methylpyrrolidine group. On the other hand, a *n*-butyl substituent introduced on the structure of **6** led to a limited reduction of binding affinity (**12**), suggesting that lipophilic groups in the proximity of the basic center could be tolerated, and leading us to focus on the butyl chain to further explore the steric requirements for this portion of the molecule.

Keeping fixed R^1 piperidine and R^3 butyl substituents, 2-methylpyrrolidine with (*R*) or (*S*) chirality was evaluated as R^2 substituent (**13–16**). The diastereomeric mixtures obtained during the synthetic procedure were separated and each stereoisomer was tested separately. Consistently with what observed for compounds **7** and **8**, (*S*)-methylpyrrolidine provided compounds with slightly higher binding affinity compared to the (*R*)-isomers. Replacement

of the (*S*)-methylpyrrolidine with a bulkier (*S*)-methylpiperidine (**17, 18**) led to lower binding affinity. In all cases both human and rat receptors showed limited and/or variable stereoselectivity for the chiral center at the benzylic carbon. This lack of stereoselectivity, probably related to chain flexibility, was further confirmed for all the couples of diastereomeric derivatives of (*S*)-methylpyrrolidine tested (*vide infra*).

R^3 bulkiness and lipophilicity were further increased with methoxypropyl (**19** and **20**), phenoxypropyl (**21** and **22**) and 4-methoxyphenoxypropyl (**23** and **24**) side chains, while keeping the R^2 substituent a (*S*)-methylpyrrolidine. The resulting compounds maintained binding affinities comparable to those of butyl derivatives **15** and **16**, reaching subnanomolar affinities for human H_3 receptor with compounds **20** and **21**. Compound **20**, with a $pK_B = 10.02$ was the most potent H_3 -antagonist in the functional assay on human receptors. These results confirmed the remarkable steric tolerance of human and rat H_3 receptors for lipophilic chains stemming out from the rigid biphenyl scaffold, in an almost-perpendicular direction with respect to the two basic groups. Finally, compounds **34** and **35**, lacking one of the cyclic amine fragment either close to the lipophilic tail or at the opposite site, were synthesized to assess the role of the two basic groups. Both these compounds showed remarkable drops in binding affinity ($pK_i < 5$), suggesting that the two basic groups are both important for binding interactions within this series.

The compounds under study were selective for H_3 receptor, showing no activity on other histamine receptors, up to micromolar concentration. In detail, compounds **7–24** did not display antagonism towards guinea-pig H_1 receptors at concentrations lower than 100-fold those required to inhibit H_3 receptors. On guinea-pig histamine H_2 receptors, compound **14** behaved as a weak competitive antagonist ($pK_B = 5.13$), while for other compounds no significant activity was detected at concentration of $1 \mu\text{M}$. All the substances showed no or negligible affinity for human H_4 receptor ($pK_i \leq 4.5$). Compound **21**, characterized by the highest hH_3 binding affinity, was also tested on bungarotoxin-sensitive nicotinic receptors. It showed no affinity for human $\alpha 7$ nicotinic receptors and only 27% displacement of radiolabelled bungarotoxin from human muscle-type nicotinic receptors at $1 \mu\text{M}$ concentration.

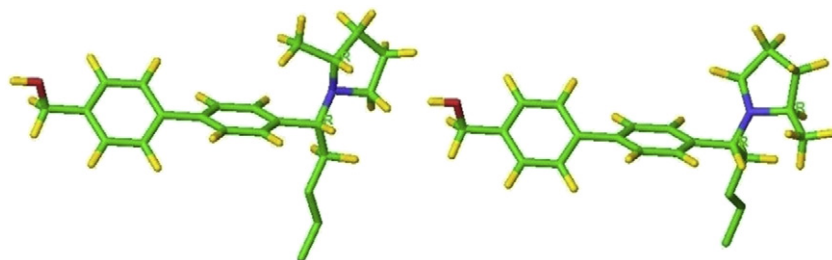
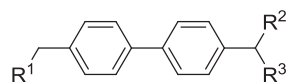


Fig. 6. Representative conformations of the (*R,R*) isomer with $\tau_1 \approx 60^\circ$ (left) or $\tau_1 \approx 180^\circ$ (right) and $\tau_2 \approx 180^\circ$.

Table 1
Binding affinity at human and rat H₃ receptor (pK_i) and antagonist potency at human H₃ receptor (pK_B) for newly synthesized compounds.



	R ¹	R ²	R ³	Stereochemical assignment ^a	hH ₃ pK _i ^b	rH ₃ pK _i ^c	hH ₃ pK _B ^d
6			-H		9.47 ²⁶	8.92 ²⁶	8.77 ⁴¹
7			-H	(R)	8.83 ± 0.10	8.45 ± 0.04	9.16 ± 0.17
8			-H	(S)	9.18 ± 0.02	9.43 ± 0.12	9.46 ± 0.39
9			-CH ₂ Ph	(±)	7.72 ± 0.08	6.95 ± 0.06	8.30 ± 0.12
10		-N(CH ₃) ₂	-CH ₂ Ph	(±)	7.78 ± 0.01	7.52 ± 0.10	7.56 ± 0.11
11			-CH ₂ Ph	(S,R)/(R,R)	8.25 ± 0.12	7.53 ± 0.16	8.87 ± 0.18
12			-(CH ₂) ₃ CH ₃	(±)	8.89 ± 0.02	8.37 ± 0.05	8.81 ± 0.16
13			-(CH ₂) ₃ CH ₃	(S,R)	8.63 ± 0.06	7.79 ± 0.03	8.58 ± 0.21
14			-(CH ₂) ₃ CH ₃	(R,R)	8.61 ± 0.07	7.90 ± 0.15	8.80 ± 0.30
15			-(CH ₂) ₃ CH ₃	(R,S)	8.81 ± 0.02	8.06 ± 0.12	8.81 ± 0.32
16			-(CH ₂) ₃ CH ₃	(S,S)	8.90 ± 0.17	8.85 ± 0.08	8.37 ± 0.43
17			-(CH ₂) ₃ CH ₃	(R,S)	8.52 ± 0.04	7.58 ± 0.01	8.91 ± 0.33
18			-(CH ₂) ₃ CH ₃	(S,S)	8.61 ± 0.13	7.58 ± 0.13	8.94 ± 0.30
19			-(CH ₂) ₃ OCH ₃	(R,S)	8.70 ± 0.09	8.83 ± 0.01	9.64 ± 0.25
20			-(CH ₂) ₃ OCH ₃	(S,S)	9.06 ± 0.14	8.75 ± 0.10	10.02 ± 0.09
21			-(CH ₂) ₃ OPh	(R,S)	9.29 ± 0.10	8.18 ± 0.10	8.48 ± 0.18
22			-(CH ₂) ₃ OPh	(S,S)	8.59 ± 0.10	8.33 ± 0.09	9.15 ± 0.18
23			-(CH ₂) ₃ O(4'OCH ₃ Ph)	(R,S)	8.90 ± 0.12	8.18 ± 0.01	8.71 ± 0.24
24			-(CH ₂) ₃ O(4'OCH ₃ Ph)	(S,S)	8.69 ± 0.10	8.68 ± 0.10	8.71 ± 0.25
34		-H	-(CH ₂) ₃ CH ₃		4.89 ± 0.09	4.22 ± 0.05	N.D.

Table 1 (continued)

	R ¹	R ²	R ³	Stereochemical assignment ^a	hH ₃ pK _i ^b	rH ₃ pK _i ^c	hH ₃ pK _B ^d
35	–H		–(CH ₂) ₃ CH ₃	(±)	4.87 ± 0.06	4.36 ± 0.05	N.D.

^a For compounds **13–24** stereochemical assignment was based on NMR analysis. Absolute configuration is reported in the order (benzylic carbon, R²).

^b Inhibition of [³H]RAMHA binding to SK-N-MC cells stably expressing the human histamine H₃ receptor.

^c Inhibition of [³H]RAMHA binding to rat brain membranes.

^d Antagonist potency at human histamine H₃ receptors expressed in SK-N-MC cells. N.D. Not determined.

Starting from previous modeling work, which had proposed the existence of two mutually perpendicular pockets into the H₃ receptor [26], we tested the possibility that those two pockets could be simultaneously fitted by our compounds. We thus built a new model of the human H₃ receptor by homology modeling, based on the three-dimensional structure of human H₁ receptor co-crystallized with the antagonist doxepin [44].

H₁ and H₃ receptors are characterized by 43% homology and 21% identity, considering their whole sequences. Although homology-based models should be regarded as heuristic, previously developed models of H₃ receptor showed acceptable performance in discriminating active from inactive compounds [32] and reproducing antagonist SARs [45], even if they had been built from less similar templates. Transmembrane (TM) sequences of H₁ and H₃ receptors show 68% homology and 36% identity of amino acids, sharing some key amino acids involved in ligand recognition. In TM3, the conserved aspartic acid (Asp107) of the H₁ crystal structure interacts with the basic nitrogen of doxepin. Asn198 in TM5 of the H₁ receptor is thought to bind the imidazole ring of the natural ligand histamine [46], while it does not interact with doxepin in the crystal structure. The corresponding amino acid in the H₃ receptor is Glu206, important for histamine and (R)- α -methylhistamine binding, as highlighted by mutagenesis studies [47]. Some other amino acids lining the doxepin binding site in the H₁ receptor are conserved in the H₃ receptor, such as Tyr108 in TM3 close to the conserved aspartic acid, Trp428 belonging to the CWXP motif in TM6, Thr112, Phe199, Phe424, and Tyr431.

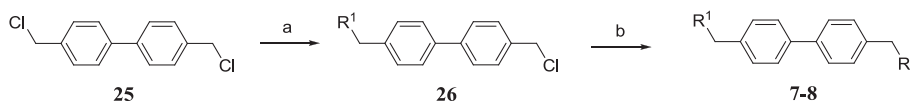
Human and rat H₃ receptors are characterized by high homology in their amino acid sequences (92% identity) and, although some molecular models had been invoked to explain different binding affinities for some H₃-antagonists [30], we did not try to rationalize the differences observed in this work given the similarity between the SARs on the receptors from the two species. Compounds **23** and **24**, with the bulkiest lipophilic chain in the series, were docked within the receptor binding site. In the best docking solutions the piperidine nitrogen of both compounds undertakes a hydrogen-bond with Glu206 in TM5 and the pyrrolidine interacts with Asp114 in TM3 (Fig. 7), similarly to what had been reported for compound **6** in its “horizontal” pose. The aromatic ring of the benzylpiperidine portion forms a π -stacking interaction with Tyr115 in TM3 (not shown), similarly to what had been described for another series of dibasic H₃-antagonists [31]. No interactions are seen with amino acids of the extracellular

loops. The 4-methoxyphenoxypropyl chains of **23** and **24** extend into the “vertical” pocket lined by TM3, TM6 and TM7, confirming that the two pockets outlined in the receptor binding site can be simultaneously occupied by the antagonists. The lack of stereoselectivity at the benzylic carbon observed throughout the series is consistent with the similar docking poses for the two stereoisomers represented in Fig. 7. Although this pose showed the highest docking score, alternative orientations for these compounds cannot be ruled out, and other docking solutions were obtained. In one pose the pyrrolidine nitrogen is bound to Asp114 and the piperidine ring is inserted into the “vertical” pocket, interacting with polar amino acids, such as Asp80 in TM2, Ser121 in TM3 and Ser405 in TM7. This pose is consistent with the “vertical” accommodation, previously found for the symmetrical derivative **6**. The two basic groups can also exchange their residue counterpart, with the pyrrolidine nitrogen interacting with Glu206 and the piperidine one with Asp114; in this case the lipophilic tail points toward the extracellular portion of the receptor. No correlation was found between hH₃ binding affinities of compounds **6–24** and the docking scores obtained from an induced-fit docking (see Supplementary Material).

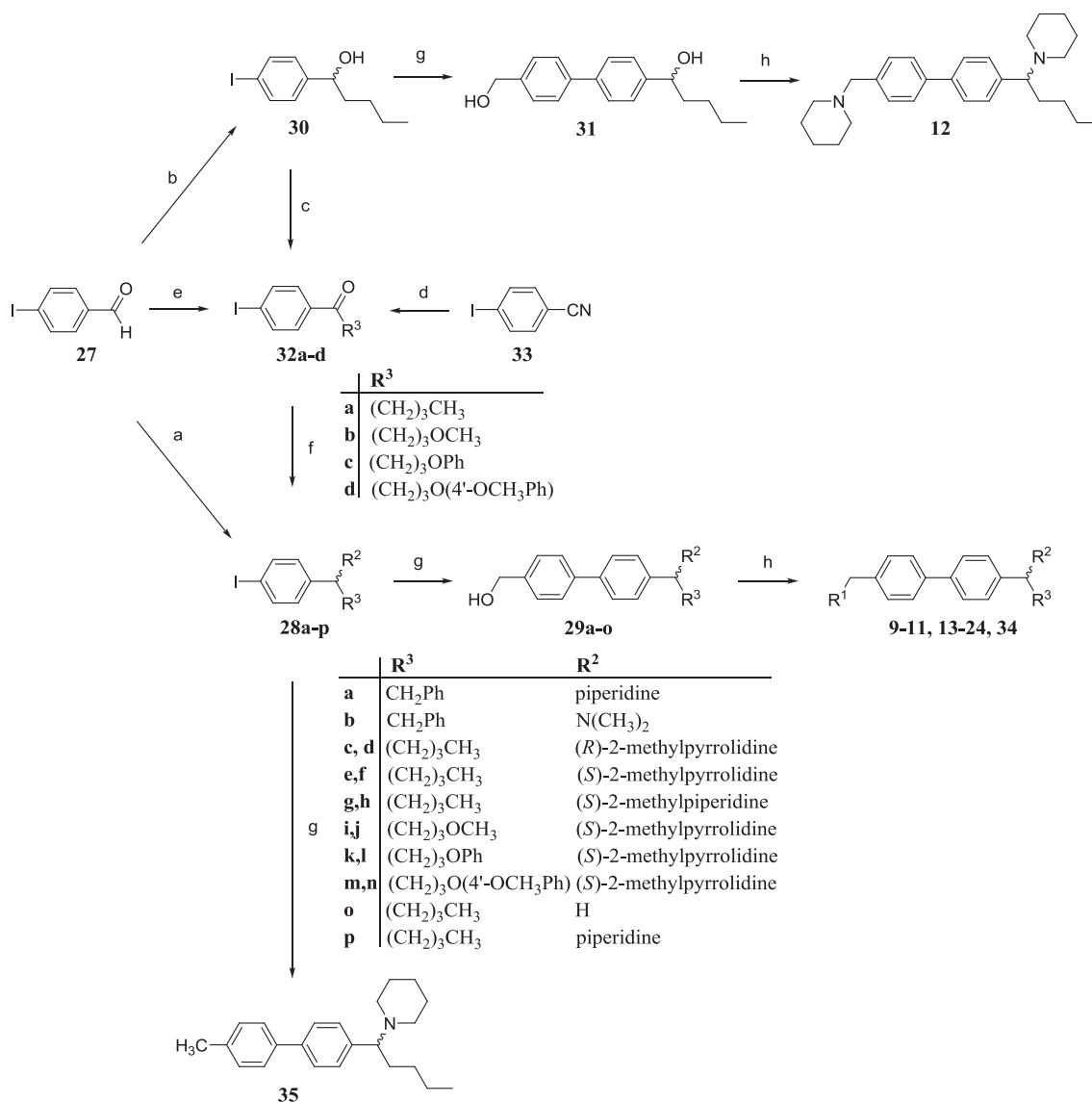
4.2. Diastereomeric characterization by NMR studies and molecular dynamics

Several new compounds were synthesized as mixtures of two diastereoisomers (**13–14**, **15–16**, **17–18**, **19–20**, **21–22**, and **23–24**) and then separated by silica gel chromatography. As only the chirality of one stereocenter was known, assignment of their absolute configuration was achieved combining high resolution (600 MHz) 1D and 2D NMR data and computational studies. To define a rule for stereochemical assignment, we focused on the intermediates **29c,d** (Fig. 3), as these compounds lack the piperidine ring, which gave NMR signals highly overlapping those of the pyrrolidine one. Compound **29c** was the isomer that eluted first, and **29d** the latter one (see Experimental Section). Complete and unambiguous assignment of all resonances was achieved by the combined analysis of 1D ¹H and ¹³C, 2D COSY, HSQC and NOESY spectra (see Experimental Section and Supporting Information, Figures S2–S5). Relevant features for stereochemical assignment are here summarized.

The ¹H NMR spectrum of compound **29c** showed a more shielded signal for proton H2a (Fig. 3), compared to the same proton of



Scheme 1. Reagents and conditions: (a) piperidine, Et₃N, CH₃CN, MW 150 °C, 150 W, 120 psi, 5 min, 48%; (b) (R)- or (S)-2-methylpyrrolidine, CH₃CN, MW 150 °C, 150 W, 120 psi, 5 min, 78–87%.



Scheme 2. Reagents and conditions: (a) i. piperidine (to **28a**) or dimethylamine (to **28b**), anhydrous CH₃CN, r.t.; ii. benzyl zinc bromide, anhydrous CH₃CN, anhydrous THF, -5 °C to r.t., 73–87%; (b) butyl magnesium bromide, anhydrous Et₂O, -5 °C to r.t., 93%; (c) PCC, CH₂Cl₂, molecular sieve 4 Å, 93% (to **32a**); (d) i. methoxypropyl magnesium chloride, I₂, anhydrous Et₂O, 16 h; ii. 6 M HCl, 68% (to **32b**); (e) allyloxybenzene derivative, 2-amino-3-picoline, benzoic acid, aniline, [Rh(PPh₃)₃Cl], anhydrous toluene, 130 °C, 1 h, 43–66% (to **32c–d**); (f) i. (*R*)- or (*S*)-2-methylpyrrolidine (to **28c–f, i–n**), (*S*)-2-methylpiperidine (to **28g–h**) or piperidine (to **28p**), Ti(Oi-Pr)₄, anhydrous THF, reflux, 16 h; ii. NaBH(OAc)₃, CH₃OH, -48 °C to r.t., 6 h, 32–85%; (g) 4-hydroxymethylphenylboronic acid (to **29a–o** and **31**) or *p*-tolylboronic acid (to **35**), Cs₂CO₃, Pd(Ac)₂, Acetone, CH₃OH, H₂O, 65 °C, 1 h or MW 100 °C, 50 W, 120 psi, 10 min, 61–92%; (h) i. MsCl, Et₃N, CH₂Cl₂, 0 °C to r.t.; ii. piperidine (to **9–10, 12–24** and **34**) or (*R*)-2-methylpyrrolidine (to **11**), Et₃N, CH₃CN, MW 100 °C, 80 W, 120 psi, 5 min, 55–89%.

29d ($\delta_{\text{H}2\text{a}} = 2.37$ and 2.97 ppm, respectively). On the other hand, ¹H NMR of **29c** showed less shielded signals for protons H6 and CH₃ (**29c**: $\delta_{\text{H}6} = 3.7$ and $\delta_{\text{CH}3} = 1.1$ ppm; **29d**: $\delta_{\text{H}6} = 3.4$ and $\delta_{\text{CH}3} = 0.82$ ppm).

In the ¹H NMR spectrum of **29c** butylic H7 protons were overlapped ($\delta_{\text{H}7\text{a},\text{H}7\text{b}} = 1.79$ – 1.89 ppm), with $^3J_{\text{H}6\text{H}7} = 9.6$ and 6.0 Hz. Peaks corresponding to H2a and H5b were sharp, with coupling constants $^3J_{\text{H}2\text{aH}3\text{a}} = ^3J_{\text{H}2\text{aH}3\text{b}} = 6.6$ Hz, and $^3J_{\text{H}5\text{bH}4} = 8.4$ and 3.0 Hz.

In the ¹H NMR spectrum of compound **29d**, butylic protons H7a and H7b gave well-defined separated signals ($\delta_{\text{H}7\text{a}} = 1.82$ and $\delta_{\text{H}7\text{b}} = 1.74$ ppm), with coupling constants toward H6 corresponding to a gauche ($^3J_{\text{H}6\text{H}7\text{a}} = 3.6$ Hz) and an anti ($^3J_{\text{H}6\text{H}7\text{b}} = 10.8$ Hz) conformation, respectively. Only proton H7b showed strong NOE signal with aromatic H12 protons, while H7a showed cross peaks to pyrrolidine protons H2a, H3a, H3b, H4a, H5a

and H5b. Pyrrolidine protons H2a and H5b showed broad signals at 2.97 and 2.76 ppm, respectively.

Molecular dynamics (MD) simulations were performed on the (*S,R*) and (*R,R*) stereoisomers of {4'-[1-(2-methylpyrrolidin-1-yl)pentyl]biphenyl-4-yl}methanol (Fig. 3), simulating the solvent effect of chloroform by a GB/SA model. 10,000 Snapshots were collected during 1 μs of simulation. The most relevant differences in conformational equilibria among the two stereoisomers regarded butyl chain and pyrrolidine rotation. For the (*S,R*) stereoisomer, the pyrrolidine adopted one preferred orientation ($\tau_1 \approx 300^\circ$ in Fig. 4A), with the methyl substituent close to the benzylic hydrogen H6 (Fig. 5). For the (*R,R*) stereoisomer, the pyrrolidine exchanged between two equally populated orientations ($\tau_1 \approx 60^\circ$ and 180° in Fig. 4C). In the first ($\tau_1 \approx 60^\circ$) the methyl substituent points toward the biphenyl scaffold (Fig. 6, left), while in the second ($\tau_1 \approx 180^\circ$) the methyl group is close to the benzylic hydrogen (Fig. 6, right).

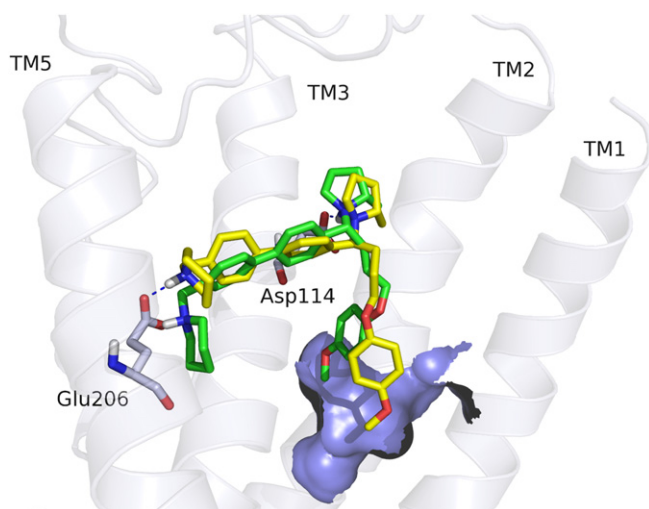


Fig. 7. Superposition of the energy-minimized H₃ receptor model-23 (green carbons) and H₃-24 (yellow carbons) complexes. Asp114 and Glu206 are depicted with gray sticks. TM6 and TM7 have been removed for clarity.

The butyl chain assumed two preferred orientations for the (*S,R*) isomer ($\tau_2 \approx 180^\circ$ and 300° in Fig. 4B), with the first rotatable bond in *anti* or *gauche* conformation (Fig. 5). On the contrary, for the (*R,R*) isomer the butyl chain orientation was almost fixed with $\tau_2 \approx 180^\circ$ (Figs. 4D and 6), with only a limited number of snapshots ($\sim 9\%$) having $\tau_2 \approx 60^\circ$.

NMR data for **29c** are in agreement with the conformational behavior of the (*S,R*) isomer. The preferred orientation of the pyrrolidine ring is supported by NOE signals involving the *ortho*-aromatic protons (H12): significant signals were observed with H2a, H5a, H5b and CH₃ protons, but not with H3a, H3b, H4a and H4b (Supporting Information, Figure S3). Consistently, average distances between H12 and H5a and H5b are 2.81 Å and 3.26 Å, respectively; average minimum distance between H12 and CH₃ protons is 3.07 Å. The two favored orientations of the butyl chain are consistent with J_{H7a-H6} and J_{H7b-H6} values, deriving from a combination of *anti* and *gauche* arrangements (Table 2).

NMR data for **29d** are in agreement with MD simulation results for the (*R,R*) isomer: the presence of one preferred conformation of the butyl chain is consistent with the J_{H7a-H6} *gauche* and J_{H7b-H6} *anti* values, as well as with the strong NOE signal between H12 and H7b, and with the lack of any NOE signal between H12 and H7a. Rotation of the pyrrolidine ring is also consistent with the high number of weak NOE signals from both the aromatic *ortho* protons (H12) and the butylic H7 protons to the pyrrolidine ones (Supporting Information, Figure S5). Moreover, other 3J values calculated for the (*S,R*) and (*R,R*) isomers were in good agreement with those observed for **29c** and **29d**, respectively (Table 2). Finally the assignment (*S,R*)-**29c** and (*R,R*)-**29d** is also consistent with the different δ values of

H2a (more shielded in **29c**) and CH₃ (more shielded in **29d**) protons. In fact, for the (*S,R*) isomer the majority of conformations had H2a above the plane of the phenyl ring (Fig. 5) while, in the case of the (*R,R*) isomer, one of the two equally preferred conformations had the CH₃ above the plane of the phenyl ring (Fig. 6).

For all couples of diastereoisomers **13–24**, the isomer eluted first from the chromatographic column (indicated as isomer A in the Experimental Section) showed NMR features resembling those of **29c** (e.g. more shielded signals for proton H2a, closer coupling constants between H6 and H7a and H7b protons), while the second eluted (isomer B) showed features of the **29d** spectrum (e.g. more shielded signals for CH₃ protons and H6, significantly different coupling constants between H6 and H7a and H7b protons). Configuration at the benzylic carbon was therefore assigned on the basis of their NMR spectra, assuming that isomer A has the two stereocenters with opposite absolute configuration. This resulted in the assignments reported in Table 1.

5. Conclusions

Starting from the structure of the lead compound **6**, we devised new H₃-antagonists characterized by two basic centers and a lipophilic side chain at the benzylic carbon linking the biphenyl scaffold to a chiral basic group. The high binding affinity and antagonist behavior shown by these compounds, including those with a bulky lipophilic chain, support the hypothesis that two previously described regions within the H₃ receptor binding site are simultaneously available for ligand binding. Stereoselectivity for diastereomeric couples with opposite chirality at the benzylic carbon was very limited or absent, probably due to the flexibility of the lipophilic substituent.

6. Experimental section

6.1. General chemistry

Microwave reactions (MW) were conducted with a CEM Discover Synthesis Unit. Reactions were monitored by TLC, on Kieselgel 60 F 254 (DC-Alufolien, Merck). Final compounds and intermediates were purified by flash chromatography, using either SiO₂ column (Prepacked Cartridges, SiO₂ 60, 40–63 μ m, BÜCHI) or prepacked silica gel cartridges (Biotage). Melting points were determined with a Gallenkamp melting point apparatus and are uncorrected. Where melting points are not indicated compounds were obtained as oils. NMR spectra were recorded on Bruker 300 Avance (300 MHz), Bruker 400 Avance (400 MHz) and Varian Inova 600 (600 MHz) spectrometers; chemical shifts (δ scale) are reported in parts per million (ppm) relative to the central peak of the solvent. ¹H NMR spectra are reported in the following order: multiplicity, approximate coupling constant (*J* value) in hertz (Hz), and number of protons; signals were characterized as s (singlet), d (doublet), dd (doublet of doublets), ddd (doublet of doublets of doublets), t (triplet), td (triplet of doublets), q (quartet), quint (quintet), sest (sestet), m (multiplet) br s (broad signal). The final compounds were analyzed on a ThermoQuest (Italia) FlahEA 1112 Elemental Analyzer, for C, H and N. The percentages we found were within $\pm 0.4\%$ of the theoretical values. Mass spectra were recorded using an API-150 EX with APCI interface (Applied Biosystem, Mds Sciex, Foster City, CA). When indicated, gaseous NH₃ was added to the methanolic phase to obtain a 5% w/w solution. Abbreviations are the following: EtOAc, ethyl acetate; THF, tetrahydrofuran; MsCl, mesyl chloride. Couples of diastereoisomers obtained as mixtures were separated by Flash Chromatography: we indicated as isomer A (ds-A) the one that eluted first, and as isomer B (ds-B) the latter one.

Table 2

¹H–¹H vicinal coupling constants (3J , Hz) observed by NMR spectroscopy (600 MHz) and calculated for (*S,R*) and (*R,R*) isomers **29c,d**.

Coupling constant	(<i>S,R</i>)-isomer		(<i>R,R</i>)-isomer	
	Measured	Calculated	Measured	Calculated
H ₂ –H _{3a}	6.6	7.1	–	–
H ₂ –H _{3b}	6.6	7.5	–	–
H _{5b} –H _{4a}	3.0	3.2	–	–
H _{5b} –H _{4b}	8.4	8.3	–	–
H _{7a} –H ₆	6.0	6.8	3.6	4.6
H _{7b} –H ₆	9.6	7.3	10.8	10.0

6.1.1. Preparation of 1-[[4'-(chloromethyl)biphenyl-4-yl]methyl]piperidine (**26**)

A solution of 4,4'-bis(chloromethyl)biphenyl **25** (1.0 mmol) in CH₃CN (3.5 mL) was reacted with piperidine (0.5 mmol) and Et₃N (0.5 mmol) (MW, 150 °C, 150 W, 120 psi, 5 min). The solvent was evaporated under reduced pressure and the residue was dissolved in CH₂Cl₂ (50 mL). The organic phase was washed with brine and dried over sodium sulfate. Removal of the solvent under reduced pressure gave the crude product, which was purified by flash chromatography (SiO₂, CH₂Cl₂/CH₃OH(NH₃) 70:1). Yield: 48%; mp: 174–176 °C. ¹H NMR (CDCl₃, 300 MHz) δ 1.52–1.40 (m, 2H), 1.64–1.57 (m, 4H), 2.43 (m, 4H), 3.56 (s, 2H), 4.63 (s, 2H), 7.41 (d, *J* = 8.2 Hz, 2H), 7.44 (d, *J* = 8.2 Hz, 2H), 7.53 (d, *J* = 8.2 Hz, 2H), 7.58 (d, *J* = 8.2 Hz, 2H). MS-(APCI): *m/z* 300.4 [M+1]⁺.

6.1.2. Preparation of (R)- and (S)-1-[[4'-(2-methylpyrrolidin-1-yl)methyl]biphenyl-4-yl]methyl]piperidine (**7–8**)

A solution of **26** (0.33 mmol) in CH₃CN (3.5 mL), was reacted with (R)- or (S)-2-methylpyrrolidine (1.00 mmol) (MW, 150 °C, 150 W, 120 psi, 5 min). CH₂Cl₂ (50 mL) was added to the reaction mixture and the organic phase was extracted with 1 M HCl aqueous solution (3 × 50 mL). The combined aqueous phases were made alkaline with K₂CO₃ and were extracted with EtOAc (3 × 50 mL). The organic layers were dried over sodium sulfate and the solvent was evaporated under reduced pressure to afford the crude products which were purified by flash chromatography (SiO₂, CH₂Cl₂/CH₃OH (NH₃) 100:1 to 80:1).

6.1.2.1. (R)-1-[[4'-(2-methylpyrrolidin-1-yl)methyl]biphenyl-4-yl]methyl]piperidine (**7**·2HCl·0.25H₂O). Yield: 87%; crystallized from abs EtOH/Et₂O; mp: >300 °C ¹H NMR (DMSO-*d*₆, 300 MHz) δ 1.28 (d, *J* = 6.5 Hz, 3H), 1.85–1.55 (m, 8H), 2.18–2.03 (m, 1H), 2.82–2.65 (m, 2H), 3.00 (sest, *J* = 8.0 Hz, 1H), 3.22–3.09 (m, 4H), 3.34 (quint, *J* = 7.3 Hz, 1H), 4.06 (dd, *J* = 12.7, 7.2 Hz, 1H), 4.17 (d, *J* = 5.1 Hz, 2H), 4.52 (dd, *J* = 13.0, 4.0 Hz, 1H), 7.69–7.60 (m, 8H), 10.76 (s, 1H). MS-(APCI): *m/z* 349.6 [M+1]⁺. Anal. Calcd for C₂₄H₃₂N₂·2HCl·0.25H₂O: C, 67.67; H, 8.16; N, 6.58. Found: C, 67.58; H, 8.12; N, 6.50.

6.1.2.2. (S)-1-[[4'-(2-methylpyrrolidin-1-yl)methyl]biphenyl-4-yl]methyl]piperidine (**8**·2HCl·0.2H₂O). Yield: 78%; crystallized from abs EtOH/Et₂O; mp: >300 °C ¹H NMR (DMSO-*d*₆, 300 MHz) δ 1.39 (d, *J* = 6.5 Hz, 3H), 1.95–1.65 (m, 8H), 2.28–2.13 (m, 1H), 2.90–2.78 (m, 2H), 3.11 (sest, *J* = 8.6 Hz, 1H), 3.32–3.20 (m, 4H), 3.45 (quint, *J* = 7.5 Hz, 1H), 4.17 (dd, *J* = 12.9, 7.1 Hz, 1H), 4.28 (d, *J* = 5.3 Hz, 2H), 4.53 (dd, *J* = 13.1, 3.7 Hz, 1H), 7.80–7.72 (m, 8H), 10.97 (s, 1H). MS-(APCI): *m/z* 349.5 [M+1]⁺. Anal. Calcd for C₂₄H₃₂N₂·2HCl·0.2H₂O: C, 67.82; H, 8.16; N, 6.59. Found: C, 67.79; H, 7.93; N, 6.50.

6.1.3. General synthesis of 1-(4-iodophenyl)-2-phenylethylamine (**28a–b**)

To a dried 100 mL flask kept under an atmosphere of argon containing zinc dust (36.8 mmol) and zinc bromide (1.2 mmol) in dry CH₃CN (16 mL), phenyl bromide (1.2 mmol) and trifluoromethanesulfonic acid (0.1 mL) were added under vigorous stirring. After 15 min, benzyl bromide (12.0 mmol) was added and the reaction mixture was stirred at room temperature for 40 min. Then the suspension was filtered over celite under nitrogen and the solution was added dropwise to a mixture of 4-iodobenzaldehyde **27** (4.0 mmol) and the appropriate amine (4.0 mmol) in dry CH₃CN (8 mL). The mixture was stirred for additional 3 h at room temperature. After completion of the reaction, 5% NaOH (50 mL) was added and the mixture was extracted with CH₂Cl₂ (3 × 50 mL). The combined organic fractions were dried over sodium sulfate and the solvent was evaporated under reduced pressure. Et₂O (50 mL) was added to the residue and concentrated H₂SO₄ (0.25 mL) was

added carefully to the vigorously stirred solution. The ether solution was taken away and the ammonium salt was washed with diethyl ether (3 × 15 mL). The residue was dissolved in 5% NaOH (35 mL) and the aqueous phase was extracted with CH₂Cl₂ (3 × 50 mL). The combined organic fractions were dried over sodium sulfate and concentrated under vacuum to give the crude products, that were purified by flash chromatography (SiO₂, CH₂Cl₂/CH₃OH (NH₃) 50:1).

6.1.3.1. (±) 1-[1-(4-iodophenyl)-2-phenylethyl]piperidine (**28a**). Yield: 87%; mp: 78–81 °C. ¹H NMR (CDCl₃, 300 MHz) δ 1.41–1.36 (m, 2H), 1.58 (m, 4H), 2.43 (m, 4H), 3.94 (dd, *J* = 13.3, 9.9 Hz, 1H), 3.32 (dd, *J* = 13.2, 4.6 Hz, 1H), 3.56 (dd, *J* = 9.6, 4.6 Hz, 1H), 6.88 (d, *J* = 8.3 Hz, 2H), 6.96 (d, *J* = 7.8 Hz, 2H), 7.17–7.06 (m, 3H), 7.55 (d, *J* = 8.2 Hz, 2H). MS-(APCI): *m/z* 392.1 [M+1]⁺.

6.1.3.2. (±) 1-(4-iodophenyl)-*N,N*-dimethyl-2-phenylethylamine (**28b**). Yield: 73%. ¹H NMR (CDCl₃, 300 MHz) δ 2.23 (s, 6H), 2.84 (dd, *J* = 13.1, 9.8 Hz, 1H), 3.27 (dd, *J* = 13.1, 4.8 Hz, 1H), 3.36 (dd, *J* = 9.7, 4.8 Hz, 1H), 6.84 (d, *J* = 8.3 Hz, 2H), 6.90 (d, *J* = 7.9 Hz, 2H), 7.15–7.05 (m, 3H), 7.25 (d, *J* = 8.31 Hz, 2H). MS-(APCI): *m/z* 352.4 [M+1]⁺.

6.1.4. Preparation of (±) 1-(4-iodophenyl)pentan-1-ol (**30**)

A solution of butyl bromide (10.5 mmol) in dry Et₂O (10 mL) was added dropwise to a suspension of magnesium turnings (10.5 mmol) in dry Et₂O (2 mL) keeping reflux under argon. The mixture was refluxed for 30 min. The solution of butyl magnesium bromide thus obtained was cooled to –5 °C and a solution of 4-iodobenzaldehyde **27** (7.0 mmol) in dry Et₂O (13 mL) was added. The mixture was stirred for 1 h at room temperature, then was poured onto ice and acidified with 6 M HCl. The organic layer was separated and the aqueous phase was extracted with Et₂O (3 × 50 mL). The organic solutions were combined, washed with 10% NaHCO₃ and brine, then dried over sodium sulfate and evaporated. The crude product was purified by flash chromatography (SiO₂, CH₂Cl₂/Hexane 1:1). Yield: 97%; mp: 38–40 °C. ¹H NMR (CDCl₃, 300 MHz) δ 0.89 (t, *J* = 6.9 Hz, 3H), 1.36–1.20 (m, 4H), 1.79–1.62 (m, 2H), 2.03 (s, 1H), 4.61 (t, *J* = 6.5 Hz, 1H), 7.09 (d, *J* = 8.2 Hz, 2H), 7.67 (d, *J* = 8.3 Hz, 2H).

6.1.5. Preparation of 1-(4-iodophenyl)pentan-1-one (**32a**)

To a solution of **30** (2.2 mmol) in CH₂Cl₂ (25 mL) were added molecular sieve 4 Å (5 g) and pyridinium chlorochromate (PCC) (4.3 mmol) and the resulting mixture was stirred at room temperature for 1 h. The suspension was then filtered over celite and the solvent was evaporated under reduced pressure. The crude product was purified by flash chromatography (SiO₂, CH₂Cl₂). Yield: 93%; mp: 62–64 °C. ¹H NMR (CDCl₃, 300 MHz) δ 0.90 (t, *J* = 7.3 Hz, 3H), 1.41 (sest, *J* = 7.6 Hz, 2H), 1.72 (quint, *J* = 7.3 Hz, 2H), 2.93 (t, *J* = 7.3 Hz, 2H), 7.68 (dd, *J* = 8.6, 2.0 Hz, 2H), 7.84 (dd, *J* = 8.6, 1.8 Hz, 2H).

6.1.6. Preparation of 1-(4-iodophenyl)-4-methoxybutan-1-one (**32b**)

To a flame-dried flask kept under argon, containing magnesium turnings (2.66 mmol) and an iodine crystal, were added with stirring dry Et₂O (1 mL) and a solution of 1-chloro-3-methoxypropane (2.62 mmol) in dry Et₂O (2 mL), the latter at a rate to maintain gentle refluxing. After the addition was completed, the mixture was refluxed for 1 h then cooled to room temperature. A solution of 4-iodobenzonitrile **33** (2.00 mmol) in dry Et₂O (5 mL) was slowly added and the resulting yellow mixture was refluxed overnight. A mixture of 6 N H₂SO₄ and ice was then added and the biphasic mixture was refluxed for 2 h. The aqueous phase of the cooled

reaction mixture was separated and extracted with Et₂O (3 × 10 mL). The organic phases were combined and dried over sodium sulfate. After evaporation of the solvent, the crude product was purified by flash chromatography (SiO₂, *n*-hexane/EtOAc 40:1). Yield: 68%; mp: 63–66 °C. ¹H NMR (CDCl₃, 300 MHz) δ 2.00 (quint, *J* = 6.0 Hz, 2H), 3.02 (t, *J* = 7.1 Hz, 2H), 3.32 (s, 3H), 3.45 (t, *J* = 6.0 Hz, 2H), 7.68 (d, *J* = 8.7 Hz, 2H), 7.82 (d, *J* = 8.2 Hz, 2H).

6.1.7. General synthesis of 1-(4-iodophenyl)-4-phenoxybutan-1-one derivatives (**32c–d**)

A mixture of **27** (2.00 mmol), 2-amino-3-picoline (0.40 mmol), benzoic acid (0.12 mmol), aniline (0.30 mmol), allyloxybenzene or 1-allyloxy-4-methoxybenzene (10.0 mmol) and toluene (370 μL) was degassed bubbling argon for 10 min, prior to the addition of Rh(PPh₃)₃Cl (0.04 mmol). The mixture was stirred at 130 °C for 1 h, then it was cooled, diluted with EtOAc (50 mL) and filtered over celite. The solvent was evaporated and the crude products were purified by flash chromatography (SiO₂, *n*-hexane/EtOAc 30:1).

6.1.7.1. 1-(4-Iodophenyl)-4-phenoxybutan-1-one (32c). Yield: 66%; mp: 74–77 °C. ¹H NMR (CDCl₃, 300 MHz) δ 2.22 (quint, *J* = 6.0 Hz, 2H), 3.16 (t, *J* = 7.1 Hz, 2H), 4.06 (t, *J* = 6.0 Hz, 2H), 6.88 (d, *J* = 7.7 Hz, 2H), 6.93 (dd, *J* = 8.4, 7.4 Hz, 1H), 7.27 (dd, *J* = 8.4, 7.5 Hz, 2H), 7.68 (d, *J* = 8.6 Hz, 2H), 7.82 (d, *J* = 8.3 Hz, 2H).

6.1.7.2. 1-(4-Iodophenyl)-4-(4-methoxyphenoxy)butan-1-one (32d). Yield: 43%; mp: 136–139 °C. ¹H NMR (CDCl₃, 300 MHz) δ 2.10 (quint, *J* = 6.2 Hz, 2H), 3.05 (t, *J* = 7.1 Hz, 2H), 3.66 (s, 3H), 3.91 (t, *J* = 6.0 Hz, 2H), 6.72 (s, 4H), 7.59 (d, *J* = 8.5 Hz, 2H), 7.73 (d, *J* = 8.5 Hz, 2H).

6.1.8. General synthesis of (4-iodophenyl)methylen amines (**28c–n,p**)

A mixture of the proper ketone **32** (0.35 mmol) and the proper secondary amine (0.42 mmol) in dry THF (3 mL) at room temperature was treated with titanium tetra-isopropoxide (0.70 mmol) under nitrogen and then stirred at 75 °C for 16 h. The reaction was cooled at –48 °C and then treated with sodium triacetoxyborohydride (0.70 mmol) followed by CH₃OH (2 mL). The resulting mixture was warmed to room temperature over 6 h. The reaction mixture was diluted with THF (10 mL) and was neutralized with 10% NaOH. After filtration over celite, the solvent was evaporated under reduced pressure. The residue was taken up in EtOAc (50 mL), washed with brine, then the organic layer was dried over sodium sulfate and concentrated under reduce pressure to give crude products which were purified by flash chromatography (SiO₂). Compounds **28c–n** were obtained as couples of diastereoisomers.

6.1.8.1. (2*R*)-1-[1-(4-Iodophenyl)pentyl]-2-methylpyrrolidine (28c–d), mixture of diastereoisomers. Starting from 1-(4-iodophenyl)pentan-1-one (**32a**) and (*R*)-2-methylpyrrolidine, compounds **28c** and **28d** were obtained, after FC purification (CH₂Cl₂/CH₃OH(NH₃) 75:1), as diastereomeric mixture observed by NMR. Reaction yield: 85%, **28c/28d** 65:35. **28c:** ¹H NMR (CDCl₃, 300 MHz) δ 0.85 (t, *J* = 8.8 Hz, 3H), 1.00 (m, 1H), 1.09 (d, *J* = 6.1 Hz, 3H), 1.30 (m, 3H), 1.53 (m, 1H), 1.75 (m, 3H), 1.88 (m, 2H), 2.33 (q, *J* = 8.5 Hz, 1H), 2.40 (q, *J* = 6.5 Hz, 1H), 2.85 (td, *J* = 7.9, 3.3 Hz, 1H), 3.65 (dd, *J* = 9.3, 5.6 Hz, 1H), 6.97 (d, *J* = 8.2 Hz, 2H), 7.64 (d, *J* = 10.5 Hz, 2H). MS-(APCI): *m/z* 392.1 [M+1]⁺. **28d:** ¹H NMR (CDCl₃, 300 MHz) δ 0.83 (t, *J* = 7.4 Hz, 3H), 0.87 (d, *J* = 5.9 Hz, 3H), 1.00 (m, 1H), 1.30 (m, 3H), 1.53 (m, 1H), 1.75 (m, 3H), 1.88 (m, 2H), 2.47 (q, *J* = 9.1 Hz, 1H), 2.80 (m, 1H), 3.00 (m, 1H), 3.37 (dd, *J* = 10.5, 3.7 Hz, 1H), 7.09 (d, *J* = 8.2 Hz, 2H), 7.63 (d, *J* = 10.7 Hz, 2H). MS-(APCI): *m/z* 392.1 [M+1]⁺.

6.1.8.2. (2*S*)-1-[1-(4-iodophenyl)pentyl]-2-methylpyrrolidine (28e–f), mixture of diastereoisomers. Starting from 1-(4-iodophenyl)pentan-1-one (**32a**) and (*S*)-2-methylpyrrolidine, and after FC purification (CH₂Cl₂/CH₃OH(NH₃) 75:1), compounds **28e** and **28f** were obtained as distereomeric mixture observed by NMR. Reaction yield: 77%, **28e/28f** 65:35. **28e:** ¹H NMR (CDCl₃, 300 MHz) δ 0.80 (t, *J* = 7.7 Hz, 3H), 1.08 (d, *J* = 6.0 Hz, 3H), 1.42–0.95 (m, 4H), 1.58–1.45 (m, 1H), 1.95–1.60 (m, 5H), 2.50–2.28 (m, 2H), 2.84 (t, *J* = 7.8 Hz, 1H), 3.64 (dd, *J* = 9.2, 5.8 Hz, 1H), 6.95 (d, *J* = 7.7 Hz, 2H), 7.63 (d, *J* = 7.4 Hz, 2H). **28f:** ¹H NMR (CDCl₃, 300 MHz) δ 0.80 (t, *J* = 7.7 Hz, 3H), 0.84 (d, *J* = 7.7 Hz, 3H), 1.42–0.95 (m, 4H), 1.58–1.45 (m, 1H), 1.95–1.60 (m, 5H), 2.50–2.28 (m, 1H), 2.80 (m, 1H), 3.00 (m, 1H), 3.36 (dd, *J* = 10.5, 3.6 Hz, 1H), 7.08 (d, *J* = 7.7 Hz, 2H), 7.62 (d, *J* = 7.6 Hz, 2H). MS-(APCI): *m/z* 392.1 [M+1]⁺.

6.1.8.3. (2*S*)-1-[1-(4-iodophenyl)pentyl]-2-methylpiperidine (28g), isomer A. Reaction of **32a** and (*S*)-2-methylpiperidine, followed by FC purification (CH₂Cl₂/CH₃OH(NH₃) 80:1) gave **28g** as a single diastereoisomer (ds-A). Reaction yield 32%, ds-A/ds-B 65:35. ¹H NMR (CDCl₃, 300 MHz) δ 0.75 (t, *J* = 7.3 Hz, 3H), 1.05–0.90 (m, 2H), 0.99 (d, *J* = 6.4 Hz, 3H), 1.35–1.10 (m, 6H), 1.72–1.40 (m, 4H), 2.07 (ddd, *J* = 7.9, 6.9, 3.6 Hz, 1H), 2.24 (ddd, *J* = 7.8, 7.7, 4.0 Hz, 1H), 2.95–2.80 (m, 1H), 3.55 (dd, *J* = 10.2, 3.2 Hz, 1H), 6.99 (d, *J* = 8.1 Hz, 2H), 7.51 (d, *J* = 8.3 Hz, 2H). MS-(APCI): *m/z* 372.2 [M+1]⁺.

6.1.8.4. (2*S*)-1-[1-(4-iodophenyl)pentyl]-2-methylpiperidine (28h), isomer B. Reaction of **32a** and (*S*)-2-methylpiperidine, followed by FC purification (CH₂Cl₂/CH₃OH(NH₃) 80:1) gave **28h** as a single diastereoisomer. Reaction yield 32%, ds-A/ds-B 65:35. ¹H NMR (CDCl₃, 300 MHz) δ 0.74 (t, *J* = 6.8 Hz, 3H), 1.05–0.92 (m, 2H), 1.04 (d, *J* = 6.1 Hz, 3H), 1.25–1.10 (m, 4H), 1.52–1.30 (m, 4H), 1.71–1.58 (m, 2H), 1.80 (t, *J* = 11.0, 10.4 Hz, 1H), 2.08–1.96 (m, 1H), 2.77 (d, *J* = 11.2 Hz, 1H), 3.78 (dd, *J* = 7.3, 6.5 Hz, 1H), 6.86 (d, *J* = 8.3 Hz, 2H), 7.52 (d, *J* = 8.3 Hz, 2H). MS-(APCI): *m/z* 372.2 [M+1]⁺.

6.1.8.5. (2*S*)-1-[1-(4-iodophenyl)-4-methoxybutyl]-2-methylpyrrolidine (28i–j), mixture of diastereoisomers. Starting from 1-(4-iodophenyl)-4-methoxybutan-1-one **32b** and (*S*)-2-methylpyrrolidine, compounds **28i** and **28j** were purified by FC (CH₂Cl₂/CH₃OH(NH₃) 100:1) to obtain the distereomeric mixture observed by NMR. Reaction yield: 64%, **28i/28j** 65:35. **28i:** ¹H NMR (CDCl₃, 300 MHz) δ 0.97 (d, *J* = 6.1 Hz, 3H), 1.35–1.10 (m, 2H), 1.48–1.35 (m, 1H), 1.72–1.50 (m, 3H), 1.90–1.72 (m, 2H), 2.30 (q, *J* = 6.5 Hz, 1H), 2.36 (q, *J* = 9.2 Hz, 1H), 2.72 (td, *J* = 7.8, 3.33 Hz, 1H), 3.18 (s, 3H), 3.23 (t, *J* = 6.5 Hz, 2H), 3.55 (dd, *J* = 8.6, 6.3 Hz, 1H), 6.85 (d, *J* = 8.2 Hz, 2H), 7.52 (d, *J* = 8.2 Hz, 2H). **28j:** ¹H NMR (CDCl₃, 300 MHz) δ 0.73 (d, *J* = 6.2 Hz, 3H), 1.35–1.10 (m, 2H), 1.48–1.35 (m, 1H), 1.72–1.50 (m, 3H), 1.90–1.72 (m, 2H), 2.20 (q, *J* = 8.2 Hz, 1H), 2.66 (m, 1H), 2.89 (m, 1H), 3.10 (s, 3H), 3.18 (t, *J* = 6.3 Hz, 2H), 3.28 (dd, *J* = 10.5, 3.6 Hz, 1H), 6.96 (d, *J* = 8.1 Hz, 2H), 7.51 (d, *J* = 8.3 Hz, 2H). MS-(APCI): *m/z* 374.1 [M+1]⁺.

6.1.8.6. (2*S*)-1-[1-(4-iodophenyl)-4-phenoxybutyl]-2-methylpyrrolidine (28k), isomer A. The title compound was prepared from 1-(4-iodophenyl)-4-phenoxybutan-1-one **32c** and (*S*)-2-methylpyrrolidine. The diastereomeric mixture was separated and **28k** isolated as a single isomer by FC (CH₂Cl₂/CH₃OH (NH₃) 70:1). Reaction yield 50%, ds-A/ds-B 65:35. ¹H NMR (CDCl₃, 300 MHz) δ 1.10 (d, *J* = 6.2 Hz, 3H), 1.42–1.27 (m, 1H), 1.57–1.50 (m, 1H), 1.82–1.57 (m, 2H), 1.96–1.85 (m, 1H), 2.13–2.03 (m, 1H), 2.31 (q, *J* = 8.2 Hz, 1H), 2.42 (sest, *J* = 6.3 Hz, 1H), 2.86 (td, *J* = 8.6, 8.0, 3.3 Hz, 1H), 3.74 (dd, *J* = 8.3, 6.5 Hz, 1H), 3.94 (t, *J* = 6.4 Hz, 2H), 6.86 (d, *J* = 8.6 Hz, 2H), 6.93 (t, *J* = 7.7 Hz, 1H), 6.98 (d, *J* = 8.3 Hz, 2H), 7.27 (dd, *J* = 8.6, 7.2 Hz, 2H), 7.64 (d, *J* = 8.2 Hz, 2H). MS-(APCI): *m/z* 436.0 [M+1]⁺.

6.1.8.7. (2*S*)-1-[1-(4-iodophenyl)-4-phenoxybutyl]-2-methylpyrrolidine (**28l**), isomer B. The title compound was prepared from 1-(4-iodophenyl)-4-phenoxybutan-1-one **32c** and (S)-2-methylpyrrolidine. The diastereomeric mixture was purified and **28l** isolated as a single isomer by FC (CH₂Cl₂/CH₃OH (NH₃) 70:1). Reaction yield 50%, ds-A/ds-B 65:35. ¹H NMR (CDCl₃, 300 MHz) δ 0.74 (t, J = 6.3 Hz, 3H), 1.57–1.25 (m, 3H), 1.70–1.57 (m, 2H), 1.86–1.70 (m, 2H), 2.05–1.93 (m, 1H), 2.38 (q, J = 7.8 Hz, 1H), 2.69 (ddd, J = 8.8, 8.0, 4.2 Hz, 1H), 2.93 (m, 1H), 3.35 (dd, J = 10.5, 3.8 Hz, 1H), 3.75 (t, J = 6.4 Hz, 2H), 6.73 (d, J = 8.7 Hz, 2H), 6.81 (d, J = 7.4 Hz, 1H), 7.00 (d, J = 8.3 Hz, 2H), 7.16 (dd, J = 8.6, 8.5 Hz, 2H), 7.52 (d, J = 8.3 Hz, 2H). MS-(APCI): *m/z* 436.2 [M+1]⁺.

6.1.8.8. (2*S*)-1-[1-(4-iodophenyl)-4-(4-methoxyphenoxy)butyl]-2-methylpyrrolidine (**28m**), isomer A. The title compound was prepared from 1-(4-iodophenyl)-4-(4-methoxyphenoxy)butan-1-one **32d** and (S)-2-methylpyrrolidine. The diastereomeric mixture was purified and **28m** isolated as a single isomer by FC (CH₂Cl₂/CH₃OH (NH₃) 70:1). Reaction yield 74%, ds-A/ds-B 65:35. ¹H NMR (CDCl₃, 300 MHz) δ 1.09 (br s, 3H), 2.15–1.20 (m, 8H), 2.52–2.20 (m, 2H), 2.95–2.70 (m, 1H), 3.80–3.70 (m, 1H), 3.76 (s, 3H), 3.87 (t, J = 6.4 Hz, 2H), 6.82–6.76 (m, 4H), 6.97 (d, J = 6.9 Hz, 2H), 7.65 (d, J = 6.9 Hz, 2H). MS-(APCI): *m/z* 466.1 [M+1]⁺.

6.1.8.9. (2*S*)-1-[1-(4-iodophenyl)-4-(4-methoxyphenoxy)butyl]-2-methylpyrrolidine (**28n**), isomer B. The title compound was prepared from 1-(4-iodophenyl)-4-(4-methoxyphenoxy)butan-1-one **32d** and (S)-2-methylpyrrolidine. The diastereomeric mixture was purified and **28n** isolated as a single isomer by FC (CH₂Cl₂/CH₃OH (NH₃) 70:1). Reaction yield 74%, ds-A/ds-B 65:35. ¹H NMR (CDCl₃, 300 MHz) δ 0.85 (d, J = 5.8 Hz, 3H), 1.60–1.35 (m, 4H), 2.15–1.60 (m, 4H), 2.58–2.42 (m, 1H), 2.90–2.70 (m, 1H), 3.15–2.95 (m, 1H), 3.45 (d, J = 7.3 Hz, 1H), 3.75 (s, 3H), 3.81 (t, J = 6.4 Hz, 2H), 6.82–6.73 (m, 4H), 7.10 (d, J = 7.1 Hz, 2H), 7.63 (d, J = 8.4 Hz, 2H). MS-(APCI): *m/z* 466.1 [M+1]⁺.

6.1.8.10. (±) 1-(1-(4-iodophenyl)pentyl)piperidine (**28p**). Starting from 1-(4-iodophenyl)pentan-1-one (**32a**) and piperidine, and after FC purification (CH₂Cl₂/CH₃OH (NH₃) 80:1), compound **28p** was obtained as racemic mixture. Yield 60%. ¹H NMR (CDCl₃, 300 MHz) δ 0.82 (t, J = 7.1 Hz, 3H), 0.97–1.16 (m, 2H), 1.19–1.37 (m, 4H), 1.45–1.59 (m, 4H), 1.65–1.86 (m, 2H), 2.31 (t, J = 5.2 Hz, 4H), 3.23 (dd, J = 9.4, 4.9 Hz, 1H), 6.95 (d, J = 8.3 Hz, 2H), 7.62 (d, J = 8.3 Hz, 2H).

6.1.9. General method for preparation of hydroxymethylbiphenyl derivatives (**29a–o**, **31**) via Suzuki coupling

A solution of the proper iodophenyl derivative **28a–o** or **30** (0.50 mmol), 4-hydroxymethylphenylboronic acid (0.55 mmol), cesium carbonate (1.50 mmol) in acetone (1.5 mL), CH₃OH (2 mL) and H₂O (2 mL) was degassed bubbling nitrogen for 10 min before the addition of Pd(OAc)₂ (0.05 mmol). The mixture was heated at 100 °C for 10 min under MW irradiation (50 W, 120 psi). After filtration over celite and evaporation of the solvent, the residue was dissolved in CH₂Cl₂ (50 mL) and extracted with 1 M HCl (3 × 50 mL). The combined aqueous layers were made alkaline with K₂CO₃ and extracted with EtOAc (3 × 50 mL). The organic phases were dried over sodium sulfate and concentrated under reduced pressure to afford the crude product that was purified by flash chromatography (SiO₂). When products were obtained as mixture of diastereoisomers, we named isomer A the one that eluted first, and isomer B the latter one.

6.1.9.1. (±) {4'-[1-(Piperidin-1-yl)-2-phenylethyl]biphenyl-4-yl} methanol (**29a**). The title compound was synthesized from **28a**. FC

purification (CH₂Cl₂/CH₃OH/CH₃OH (NH₃) 50:0.9:0.1) gave the desired product. Yield: 84%. ¹H NMR (CDCl₃, 300 MHz) δ 1.43–1.35 (m, 2H), 1.68–1.56 (m, 4H), 2.32 (t, J = 5.8 Hz, 1H), 2.52–2.48 (m, 4H), 3.06 (dd, J = 13.3, 9.6 Hz, 1H), 3.36 (dd, J = 13.3, 4.9 Hz, 1H), 3.67 (dd, J = 9.5, 5.0 Hz, 1H), 4.73 (d, J = 5.6, 2H), 7.03 (d, J = 8.1 Hz, 2H), 7.18–7.06 (m, 3H), 7.21 (d, J = 8.2 Hz, 2H), 7.43 (d, J = 8.3 Hz, 2H), 7.48 (d, J = 8.2 Hz, 2H), 7.58 (d, J = 8.2 Hz, 2H). MS-(APCI): *m/z* 372.3 [M+1]⁺.

6.1.9.2. (±) {4'-[1-(dimethylamino-2-phenylethyl)biphenyl-4-yl]methanol (**29b**). The title compound was synthesized from **28b**. FC purification (CH₂Cl₂/CH₃OH/CH₃OH (NH₃) 50:0.9:0.1) gave the desired product. Yield: 90%; mp: 100–102 °C. ¹H NMR (CDCl₃, 300 MHz) δ 2.30 (s, 6H), 3.00 (dd, J = 13.3, 9.7 Hz, 1H), 3.35 (dd, J = 11.0, 4.9 Hz, 1H), 3.53 (dd, J = 9.7, 4.9 Hz, 1H), 4.74 (s, 2H), 7.03 (d, J = 8.1 Hz, 2H), 7.19–7.10 (m, 3H), 7.21 (d, J = 8.2 Hz, 2H), 7.43 (d, J = 8.3 Hz, 2H), 7.48 (d, J = 8.2 Hz, 2H), 7.58 (d, J = 8.2 Hz, 2H). MS-(APCI): *m/z* 332.2 [M+1]⁺.

6.1.9.3. {4'-[1-((R)-2-methylpyrrolidin-1-yl)pentyl]biphenyl-4-yl} methanol (**29c**), isomer A. The title compound was synthesized from **28c–d**. FC purification (CH₂Cl₂/Acetone/CH₃OH (NH₃) 15:2:0.1) gave the desired product as a single diastereoisomer. Reaction yield 84%, ds-A/ds-B 65:35. ¹H NMR (CDCl₃, 600 MHz) δ 0.79 (t, J = 7.2 Hz, 3H), 1.02–1.07 (m, 1H), 1.08 (d, J = 6.0 Hz, 3H), 1.13–1.18 (m, 1H), 1.20–1.28 (m, 1H), 1.28–1.34 (m, 1H), 1.44–1.49 (m, 1H), 1.60–1.72 (m, 1H), 1.67–1.73 (m, 1H), 1.79–1.89 (m, 2H), 2.35 (ddd like a q, J = 8.4 Hz, 1H), 2.37 (ddd, J = 7.2, 6.6, 6.0 Hz, 1H), 2.84 (td, J = 8.4, 3.0 Hz, 1H), 3.69 (dd, J = 9.6, 6.0 Hz, 1H), 4.64 (s, 2H), 7.20 (d, J = 7.8 Hz, 2H), 7.36 (d, J = 9.0 Hz, 2H), 7.48 (d, J = 8.4 Hz, 2H), 7.53 (d, J = 8.4 Hz, 2H). MS-(APCI): *m/z* 338.5 [M+1]⁺.

6.1.9.4. {4'-[1-((R)-2-methylpyrrolidin-1-yl)pentyl]biphenyl-4-yl} methanol (**29d**), isomer B. The title compound was synthesized from **28c–d**. FC purification (CH₂Cl₂/Acetone/CH₃OH (NH₃) 15:2:0.1) gave the desired product as a single diastereoisomer. Reaction yield 84%, ds-A/ds-B 65:35. ¹H NMR (CDCl₃, 600 MHz) δ 0.75 (t, J = 7.4 Hz, 3H), 0.82 (d, J = 6.3 Hz, 3H), 0.90–1.02 (m, 2H), 1.15–1.28 (m, 2H), 1.31–1.36 (m, 1H), 1.55–1.62 (m, 1H), 1.63–1.70 (m, 1H), 1.71–1.77 (m, 1H), 1.81–1.87 (m, 2H), 2.11 (m, 1H), 2.44 (ddd like a q, J = 8.4 Hz, 1H), 2.72–2.80 (m, 1H), 2.94–3.00 (m, 1H), 3.40 (dd, J = 10.8, 3.6 Hz, 1H), 4.64 (s, 2H), 7.29 (d, J = 7.8 Hz, 2H), 7.35 (d, J = 7.8 Hz, 2H), 7.45 (d, J = 7.8 Hz, 2H), 7.52 (d, J = 8.4 Hz, 2H). MS-(APCI): *m/z* 338.7 [M+1]⁺.

6.1.9.5. {4'-[1-((S)-2-methylpyrrolidin-1-yl)pentyl]biphenyl-4-yl} methanol (**29e**), isomer A. The title compound was synthesized from **28e–f**. FC purification (CH₂Cl₂/Acetone/CH₃OH (NH₃) 15:2:0.1) gave the desired product as a single diastereoisomer. Reaction yield 86%, ds-A/ds-B 65:35. ¹H NMR (CDCl₃, 300 MHz) δ 0.85 (t, J = 7.4 Hz, 3H), 1.18 (d, J = 6.2 Hz, 3H), 1.20–1.15 (m, 1H), 1.45–1.25 (m, 4H), 1.62–1.48 (m, 1H), 1.85–1.65 (m, 2H), 1.93–1.86 (m, 2H), 2.45 (q, J = 8.8 Hz, 1H), 2.46 (q, J = 5.9 Hz, 1H), 2.93 (td, J = 8.2, 3.1 Hz, 1H), 3.27 (m, 1H), 3.78 (dd, J = 8.9, 6.0 Hz, 1H), 4.71 (s, 2H), 7.28 (d, J = 8.2 Hz, 2H), 7.43 (d, J = 8.1 Hz, 2H), 7.55 (d, J = 8.2 Hz, 2H), 7.59 (d, J = 8.3 Hz, 2H). MS-(APCI): *m/z* 338.3 [M+1]⁺.

6.1.9.6. {4'-[1-((S)-2-methylpyrrolidin-1-yl)pentyl]biphenyl-4-yl} methanol (**29f**), isomer B. The title compound was synthesized from **28e–f**. FC purification (CH₂Cl₂/Acetone/CH₃OH (NH₃) 15:2:0.1) gave the desired product as a single diastereoisomer. Reaction yield 86%, ds-A/ds-B 65:35. ¹H NMR (CDCl₃, 300 MHz) δ 0.82 (t, J = 7.2 Hz, 3H), 0.96 (d, J = 6.3 Hz, 3H), 1.10–0.95 (m, 2H),

1.37–1.21 (m, 3H), 1.55–1.42 (m, 1H), 2.05–1.68 (m, 5H), 2.70–2.50 (m, 1H), 3.28–2.85 (m, 2H), 3.57 (t, $J = 6.7$ Hz, 1H), 4.74 (s, 2H), 7.43 (d, $J = 8.1$ Hz, 4H), 7.56 (d, $J = 8.5$ Hz, 2H), 7.61 (d, $J = 8.2$ Hz, 2H). MS-(APCI): m/z 338.5 [M+1]⁺.

6.1.9.7. *{4'-[1-((S)-2-methylpiperidin-1-yl)pentyl]biphenyl-4-yl}methanol (29g), isomer A.* The title compound was synthesized from **28g**. FC purification (CH₂Cl₂/CH₃OH (NH₃) 70:1) gave the desired product. Yield: 70%. ¹H NMR (CDCl₃, 300 MHz) δ 0.76 (t, $J = 7.2$ Hz, 3H), 1.10–0.90 (m, 2H), 1.05 (d, $J = 6.4$ Hz, 3H), 1.38–1.15 (m, 6H), 1.55–1.45 (m, 1H), 1.80–1.50 (m, 3H), 2.16 (ddd, $J = 10.0$, 6.5, 3.6 Hz, 1H), 2.36 (ddd, $J = 8.5$, 7.3, 3.4 Hz, 1H), 2.52 (br s, 1H), 2.98–2.85 (m, 1H), 3.70 (dd, $J = 10.1$, 3.5 Hz, 1H), 4.61 (s, 2H), 7.31 (d, $J = 8.2$ Hz, 2H), 7.32 (d, $J = 8.3$ Hz, 2H), 7.43 (d, $J = 8.3$ Hz, 2H), 7.50 (d, $J = 8.2$ Hz, 2H). MS-(APCI): m/z 352.5 [M+1]⁺.

6.1.9.8. *{4'-[1-((S)-2-methylpiperidin-1-yl)pentyl]biphenyl-4-yl}methanol (29h), isomer B.* The title compound was synthesized from **28h**. FC purification (CH₂Cl₂/CH₃OH (NH₃) 70:1) gave the desired product. Yield: 72%. ¹H NMR (CDCl₃, 300 MHz) δ 0.77 (t, $J = 7.3$ Hz, 3H), 1.12–0.95 (m, 2H), 1.12 (d, $J = 6.1$ Hz, 3H), 1.28–1.12 (m, 4H), 1.55–1.32 (m, 4H), 1.76 (q, $J = 7.3$ Hz, 2H), 1.90 (t, $J = 10.5$ Hz, 1H), 2.09 (m, 1H), 2.09 (s, 1H), 2.88 (d, $J = 11.0$ Hz, 1H), 3.91 (t, $J = 7.1$ Hz, 1H), 4.64 (s, 2H), 7.19 (d, $J = 8.1$ Hz, 2H), 7.33 (d, $J = 8.2$ Hz, 2H), 7.44 (d, $J = 8.3$ Hz, 2H), 7.51 (d, $J = 8.2$ Hz, 2H). MS-(APCI): m/z 352.5 [M+1]⁺.

6.1.9.9. *{4'-[4-methoxy-1-((S)-2-methylpyrrolidin-1-yl)butyl]biphenyl-4-yl}methanol (29i), isomer A.* The title compound was synthesized from **28i-j**. FC purification (CH₂Cl₂/CH₃OH (NH₃) 40:1) gave the desired product as single diastereoisomer. Reaction yield 92%, ds-A/ds-B 65:35. ¹H NMR (CDCl₃, 300 MHz) δ 1.05 (d, $J = 6.1$ Hz, 3H), 1.38–1.25 (m, 2H), 1.50–1.38 (m, 2H), 1.72–1.53 (m, 2H), 1.98–1.72 (m, 2H), 2.32 (q, $J = 7.8$ Hz, 1H), 2.38 (q, $J = 6.3$ Hz, 1H), 2.68 (br s, 1H), 2.81 (td, $J = 8.0$, 3.2 Hz, 1H), 3.18 (s, 3H), 3.25 (t, $J = 6.6$ Hz, 1H), 3.68 (dd, $J = 9.0$, 6.1 Hz, 1H), 4.67 (s, 2H), 7.17 (d, $J = 8.0$ Hz, 2H), 7.32 (d, $J = 8.2$ Hz, 2H), 7.44 (d, $J = 8.2$ Hz, 2H), 7.48 (d, $J = 8.2$ Hz, 2H). MS-(APCI): m/z 354.2 [M+1]⁺.

6.1.9.10. *{4'-[4-methoxy-1-((S)-2-methylpyrrolidin-1-yl)butyl]biphenyl-4-yl}methanol (29j), isomer B.* The title compound was synthesized from **28i-j**. FC purification (CH₂Cl₂/CH₃OH (NH₃) 40:1) gave the desired product as single diastereoisomer. Reaction yield 92%, ds-A/ds-B 65:35. ¹H NMR (CDCl₃, 300 MHz) δ 0.78 (d, $J = 6.2$ Hz, 3H), 1.38–1.16 (m, 3H), 1.96–1.50 (m, 5H), 2.41 (q, $J = 7.8$ Hz, 1H), 2.71 (ddd, $J = 9.1$, 7.9, 4.3 Hz, 1H), 3.00–2.90 (m, 1H), 3.03 (br s, 1H), 3.16 (s, H), 3.20 (t, $J = 6.6$ Hz, 2H), 3.37 (dd, $J = 10.6$, 3.5 Hz, 1H), 4.58 (s, 2H), 7.26 (d, $J = 8.3$ Hz, 2H), 7.30 (d, $J = 7.8$ Hz, 2H), 7.41 (d, $J = 8.3$ Hz, 2H), 7.47 (d, $J = 8.2$ Hz, 2H). MS-(APCI): m/z 354.1 [M+1]⁺.

6.1.9.11. *{4'-[1-((S)-2-methylpyrrolidin-1-yl)-4-phenoxybutyl]biphenyl-4-yl}methanol (29k), isomer A.* The title compound was synthesized from **28k**. FC purification (CH₂Cl₂/CH₃OH (NH₃) 80:1) gave the desired product. Yield: 61%. ¹H NMR (CDCl₃, 300 MHz) δ 1.09 (d, $J = 6.1$ Hz, 3H), 1.36–1.24 (m, 1H), 1.55–1.40 (m, 1H), 1.77–1.55 (m, 2H), 2.13–1.87 (m, 2H), 2.32 (q, $J = 8.3$ Hz, 1H), 2.40 (q, $J = 6.4$ Hz, 1H), 2.61 (br s, 1H), 2.84 (td, $J = 8.0$, 3.1 Hz, 1H), 3.77 (dd, $J = 8.8$, 6.2 Hz, 1H), 3.86 (t, $J = 6.5$ Hz, 2H), 4.64 (s, 2H), 6.78 (d, $J = 8.8$ Hz, 2H), 6.84 (t, $J = 7.3$ Hz, 1H), 7.18 (dd, $J = 8.5$, 7.4 Hz, 2H), 7.21 (d, $J = 8.3$ Hz, 2H), 7.36 (d, $J = 8.2$ Hz, 2H), 7.47 (d, $J = 8.2$ Hz, 2H), 7.51 (d, $J = 8.3$ Hz, 2H). MS-(APCI): m/z 416.3 [M+1]⁺.

6.1.9.12. *{4'-[1-((S)-2-methylpyrrolidin-1-yl)-4-phenoxybutyl]biphenyl-4-yl}methanol (29l), isomer B.* The title compound was synthesized

from **28l**. FC purification (CH₂Cl₂/CH₃OH (NH₃) 80:1) gave the desired product. Yield: 63%. ¹H NMR (CDCl₃, 300 MHz) δ 0.80 (d, $J = 6.3$ Hz, 3H), 1.40–1.26 (m, 1H), 1.52–1.40 (m, 2H), 1.75–1.52 (m, 2H), 1.95–1.75 (m, 2H), 2.13–1.98 (m, 1H), 2.41 (br s, 1H), 2.46 (ddd, $J = 9.1$, 7.8, 7.7 Hz, 1H), 2.76 (ddd, $J = 9.1$, 7.7, 3.9 Hz, 1H), 2.99 (m, 1H), 3.46 (dd, $J = 10.5$, 3.6 Hz, 1H), 3.79 (t, $J = 6.5$ Hz, 1H), 4.74 (s, 2H), 6.76 (d, $J = 8.6$ Hz, 2H), 6.82 (t, $J = 7.3$ Hz, 1H), 7.16 (dd, $J = 8.4$, 7.7 Hz, 2H), 7.31 (d, $J = 8.0$ Hz, 2H), 7.33 (d, $J = 7.8$ Hz, 2H), 7.44 (d, $J = 8.3$ Hz, 2H), 7.50 (d, $J = 8.2$ Hz, 2H). MS-(APCI): m/z 416.3 [M+1]⁺.

6.1.9.13. *{4'-[4-(4-Methoxyphenoxy)-1-((S)-2-methylpyrrolidin-1-yl)butyl]biphenyl-4-yl}methanol (29m), isomer A.* The title compound was synthesized from **28m**. FC purification (CH₂Cl₂/CH₃OH (NH₃) 80:1) gave the desired product. Yield 72%; ¹H NMR (CDCl₃, 300 MHz) δ 1.07 (d, $J = 6.0$ Hz, 3H), 1.34–1.22 (m, 1H), 1.55–1.38 (m, 1H), 1.74–1.53 (m, 4H), 2.10–1.85 (m, 2H), 2.27 (br s, 1H), 2.45–2.26 (m, 2H), 2.83 (td, $J = 8.0$, 3.0 Hz, 1H), 3.65 (s, 3H), 3.75 (dd, $J = 8.7$, 6.3 Hz, 1H), 3.80 (t, $J = 6.5$ Hz, 2H), 4.63 (s, 2H), 6.71 (s, 4 H), 7.20 (d, $J = 8.1$ Hz, 2H), 7.33 (d, $J = 8.2$ Hz, 2H), 7.46 (d, $J = 8.2$ Hz, 2H), 7.50 (d, $J = 8.2$ Hz, 2H). MS-(APCI): m/z 446.1 [M+1]⁺.

6.1.9.14. *{4'-[4-(4-Methoxyphenoxy)-1-((S)-2-methylpyrrolidin-1-yl)butyl]biphenyl-4-yl}methanol (29n), isomer B.* The title compound was synthesized from **28n**. FC purification (CH₂Cl₂/CH₃OH (NH₃) 80:1) gave the desired product. Yield: 71%. ¹H NMR (CDCl₃, 300 MHz) δ 0.80 (d, $J = 6.2$ Hz, 3H), 1.38–1.28 (m, 1H), 1.52–1.38 (m, 2H), 1.74–1.52 (m, 2H), 1.93–1.78 (m, 2H), 2.12–1.98 (m, 1H), 2.45 (q, $J = 7.8$ Hz, 1H), 2.55 (br s, 1H), 2.80–2.70 (m, 1H), 3.03–2.93 (m, 1H), 3.44 (dd, $J = 10.6$, 3.5 Hz, 1H), 3.65 (s, 3H), 3.74 (t, $J = 6.4$ Hz, 2H), 4.62 (s, 2H), 6.70 (s, 4 H), 7.30 (d, $J = 7.8$ Hz, 2H), 7.33 (d, $J = 7.7$ Hz, 2H), 7.43 (d, $J = 8.3$ Hz, 2H), 7.59 (d, $J = 8.2$ Hz, 2H). MS-(APCI): m/z 446.3 [M+1]⁺.

6.1.9.15. *{4'-pentylbiphenyl-4-yl}methanol (29o).* The title compound was synthesized from commercially available **28o**. FC purification (CH₂Cl₂/CH₃OH 30:1) gave the desired product. Yield: 41%; mp (*n*-hexane): 103–104 °C (*lit.* 103.5 °C)[48]. ¹H NMR (CDCl₃, 400 MHz) δ 0.91 (t, $J = 5.8$ Hz, 3H), 1.36 (m, 4H), 1.65 (quint, $J = 6.4$ Hz, 2H), 2.64 (t, $J = 7.9$ Hz, 2H), 4.74 (s, 2H), 7.25 (d, $J = 7.8$ Hz, 2H), 7.43 (d, $J = 7.8$ Hz, 2H), 7.51 (d, $J = 7.9$ Hz, 2H), 7.59 (d, $J = 8.2$ Hz, 2H).

6.1.11.16. (\pm) *1-[4'-(Hydroxymethyl)biphenyl-4-yl]pentan-1-ol (31).* The title compound was synthesized from **30**. FC purification (CH₂Cl₂/CH₃OH/CH₃OH(NH₃) 30:1:0.2) gave the desired product. Yield: 85%. ¹H NMR (CDCl₃, 300 MHz) δ 0.90 (t, $J = 6.9$ Hz, 3H), 1.46–1.24 (m, 4H), 1.87–1.69 (m, 4H), 4.71 (t, $J = 7.0$ Hz, 1H), 4.74 (s, 2H), 7.41 (d, $J = 8.0$ Hz, 2H), 7.44 (d, $J = 8.1$ Hz, 2H), 7.57 (d, $J = 8.2$ Hz, 2H), 7.59 (d, $J = 8.2$ Hz, 2H).

6.1.10. General synthesis of aminomethylbiphenyl derivatives (9–24, and 34)

To a stirred solution of hydroxymethylbiphenyl derivative **29a–o** or **31** (0.47 mmol) in CH₂Cl₂ (15 mL), MsCl (0.50 mmol for compound **31**) was added. After cooling to 0 °C, Et₃N (0.60 mmol for compounds **29a–o**, or 1.20 mmol for compound **31**) was added and the mixture was stirred at room temperature for 90 min. The solvent was evaporated to dryness and piperidine or 2-methylpyrrolidine (4.70 mmol) was added to the crude product dissolved in CH₃CN (3 mL). The mixture was heated under MW irradiation at 100 °C for 5 min (80 W, 120 psi). After cooling, CH₃CN was evaporated and the residue was taken up in CH₂Cl₂ (40 mL) and was extracted with 1 M HCl (3 \times 50 mL). The aqueous phases were made alkaline with K₂CO₃ and were extracted with EtOAc (3 \times 50 mL). The organic layers were dried over sodium sulfate and the solvent was

evaporated under reduced pressure to afford the crude products which were purified by flash chromatography (SiO₂, CH₂Cl₂/CH₃OH (NH₃) 50:1).

6.1.10.1. (\pm) 1-[[4'-(1-((S)-2-methylpyrrolidin-1-yl)methyl)biphenyl-4-yl]ethyl]piperidine (**9**·2HCl·H₂O). The compound was synthesized from **29a**. Yield: 89%; crystallized from abs EtOH/Et₂O; mp: 123 °C (dec). ¹H NMR (D₂O, 300 MHz) δ 1.46–1.27 (m, 2H), 1.95–1.57 (m, 10H), 2.94–2.74 (m, 4H), 3.50–3.37 (m, 4H), 3.60 (dd, *J* = 13.2, 4.0 Hz, 1H), 3.72 (d, *J* = 11.6 Hz, 1H), 4.24 (s, 2H), 4.62 (dd, *J* = 11.8, 3.8 Hz, 1H), 7.13–7.05 (m, 5H), 7.50–7.42 (m, 8H). MS-(APCI): *m/z* 439.3 [M+1]⁺. Anal. Calcd for C₃₁H₃₈N₂·2HCl·H₂O: C, 70.91; H, 7.99; N, 5.29. Found: C, 70.13; H, 7.86; N, 5.22.

6.1.10.2. (\pm) *N,N*-dimethyl-2-phenyl-1-[4'-(piperidin-1-ylmethyl)biphenyl-4-yl]ethanamine (**10**·2H₂SO₄). The compound was synthesized from **29b**. Yield: 60%; crystallized from Et₂O; mp: 148–153 °C. ¹H NMR (CDCl₃, 300 MHz) δ 1.46 (m, 2H), 1.63 (m, 4H), 2.32 (s, 6H), 2.45 (m, 4H), 3.02 (dd, *J* = 13.1, 9.8 Hz, 1H), 3.36 (dd, *J* = 13.3, 4.6 Hz, 1H), 3.55–3.51 (m, 1H), 3.55 (s, 2H), 7.00 (d, *J* = 6.7 Hz, 2H), 7.16–7.10 (m, 3H), 7.20 (d, *J* = 8.1 Hz, 2H), 7.40 (d, *J* = 7.9 Hz, 2H), 7.50 (d, *J* = 8.0 Hz, 2H), 7.56 (d, *J* = 8.0 Hz, 2H). MS-(APCI): *m/z* 399.4 [M+1]⁺. Anal. Calcd for C₂₈H₃₄N₂·2H₂SO₄: C, 56.55; H, 6.44; N, 4.71. Found: C, 56.60; H, 6.52; N, 4.71.

6.1.10.3. 1-[[4'-((R)-2'-methylpyrrolidin-1-yl)methyl]biphenyl-4-yl]-2-phenylethyl]piperidine (**11**·2HCl·0.8H₂O). The compound was obtained from **29a** as a 1:1 mixture of diastereoisomers. Yield: 67%; crystallized from abs EtOH/Et₂O; mp: 197 °C (dec). ¹H NMR (DMSO-*d*₆, 300 MHz) δ 1.36 (d, *J* = 6.2 Hz, 3H), 1.95–1.60 (m, 6H), 2.28–2.03 (m, 2H), 2.65–2.55 (m, 2H), 3.15–3.04 (m, 1H), 3.30–3.18 (m, 1H), 3.61–3.40 (m, 5H), 3.78 (d, *J* = 11.3 Hz, 1H), 3.86 (d, *J* = 12.0 Hz, 1H), 4.17 (dd, *J* = 12.9, 6.9 Hz, 1H), 4.52 (dd, *J* = 12.6, 3.4 Hz, 1H), 4.72 (d, *J* = 11.8 Hz, 1H), 7.17–7.08 (m, 5H), 7.80–7.60 (m, 8H), 11.00 (s, 1H), 11.45 (s, 1H). MS-(APCI): *m/z* 439.4 [M+1]⁺. Anal. Calcd for C₃₁H₃₈N₂·2HCl·0.8H₂O: C, 70.79; H, 7.97; N, 5.33. Found: C, 70.62; H, 8.01; N, 5.16.

6.1.10.4. (\pm) 1-[[4'-(1-(Piperidin-1-yl)pentyl)biphenyl-4-yl]methyl]piperidine (**12**·1.9H₂SO₄). The compound was synthesized from **31**. Yield: 85%; crystallized from Et₂O; mp: 158 °C. ¹H NMR (CDCl₃, 300 MHz) δ 0.85 (t, *J* = 7.0 Hz, 3H), 1.50–1.04 (m, 8H), 1.65–1.52 (m, 8H), 2.00–1.80 (m, 2H), 2.42 (m, 8H), 3.39 (dd, *J* = 9.1, 4.9 Hz, 1H), 3.53 (s, 2H), 7.28 (d, *J* = 8.1 Hz, 2H), 7.38 (d, *J* = 8.1 Hz, 2H), 7.56 (d, *J* = 8.2 Hz, 2H), 7.57 (d, *J* = 8.2 Hz, 2H). MS-(APCI): *m/z* 405.7 [M+1]⁺. Anal. Calcd for C₂₈H₄₀N₂·1.9H₂SO₄: C, 56.90; H, 7.47; N, 4.74. Found: C, 56.99; H, 7.98; N, 4.29.

6.1.10.5. 1-[[4'-(1-((R)-2-methylpyrrolidin-1-yl)pentyl)biphenyl-4-yl]methyl]piperidine (**13**·1.7H₂SO₄), isomer A. The compound was synthesized from **29c**. Yield: 67%; crystallized from Et₂O; mp: 187–191 °C (dec). ¹H NMR (CDCl₃, 300 MHz) δ 0.87 (t, *J* = 6.9 Hz, 3H), 1.16 (d, *J* = 6.0 Hz, 3H), 1.23–1.12 (m, 2H), 1.53–1.25 (m, 4H), 1.65–1.53 (m, 6H), 1.80–1.65 (m, 2H), 1.95–1.87 (m, 2H), 2.46 (m, 6H), 2.94 (td, *J* = 8.6, 2.9 Hz, 1H), 3.52 (s, 2H), 3.78 (dd, *J* = 8.7, 6.3 Hz, 1H), 7.27 (d, *J* = 8.1 Hz, 2H), 7.38 (d, *J* = 8.3 Hz, 2H), 7.56 (d, *J* = 7.3 Hz, 4H). MS-(APCI): *m/z* 405.2 [M+1]⁺. Anal. Calcd for C₂₈H₄₀N₂·1.7H₂SO₄: C, 58.86; H, 7.66; N, 4.90. Found: C, 58.98; H, 7.90; N, 4.66.

6.1.10.6. 1-[[4'-(1-((R)-2-methylpyrrolidin-1-yl)pentyl)biphenyl-4-yl]methyl]piperidine (**14**·2H₂SO₄·0.5H₂O), isomer B. The compound was synthesized from **29d**. Yield: 66%; crystallized from Et₂O; mp: 140–143 °C (dec). ¹H NMR (CDCl₃, 300 MHz) δ 0.85 (t, *J* = 7.2 Hz, 3H), 0.90 (d, *J* = 6.2 Hz, 3H), 1.12–1.00 (m, 2H),

1.35–1.20 (m, 2H), 1.50–1.38 (m, 3H), 1.66–1.56 (m, 4H), 1.96–1.58 (m, 5H), 2.48–2.38 (m, 4H), 2.54 (q, *J* = 7.9 Hz, 1H), 2.88 (td, *J* = 8.3, 3.5 Hz, 1H), 3.05 (q, *J* = 6.2 Hz, 1H), 3.49 (dd, *J* = 10.4, 3.8 Hz, 1H), 3.53 (s, 2H), 7.38 (d, *J* = 7.2 Hz, 4H), 7.56 (d, *J* = 8.0 Hz, 2H), 7.58 (d, *J* = 8.1 Hz, 2H). MS-(APCI): *m/z* 405.7 [M+1]⁺. Anal. Calcd for C₂₈H₄₀N₂·2H₂SO₄·0.5H₂O: C, 55.15; H, 7.44; N, 4.59. Found: C, 55.00; H, 7.49; N, 4.75.

6.1.10.7. 1-[[4'-(1-((S)-2-methylpyrrolidin-1-yl)pentyl)biphenyl-4-yl]methyl]piperidine (**15**·1.65H₂SO₄), isomer A. The compound was synthesized from **29e**. Yield: 59%; crystallized from Et₂O; mp: 160–164 °C. ¹H NMR (DMSO-*d*₆, 300 MHz) δ 0.80 (t, *J* = 7.1 Hz, 3H), 1.40–0.85 (m, 6H), 1.78–1.40 (m, 5H), 1.95–1.85 (m, 2H), 2.20–2.00 (m, 3H), 3.10–2.80 (m, 4H), 3.60–3.10 (m, 6H), 4.22–4.05 (m, 2H), 4.40–4.20 (m, 1H), 7.54 (d, *J* = 8.1 Hz, 2H), 7.50 (d, *J* = 8.1 Hz, 2H), 7.78 (d, *J* = 8.0 Hz, 2H), 7.79 (d, *J* = 8.0 Hz, 2H), 9.54 (s, 1H). MS-(APCI): *m/z* 405.8 [M+1]⁺. Anal. Calcd for C₂₈H₄₀N₂·1.65H₂SO₄: C, 59.37; H, 7.70; N, 4.94. Found: C, 59.25; H, 8.07; N, 4.84.

6.1.10.8. 1-[[4'-(1-((S)-2-methylpyrrolidin-1-yl)pentyl)biphenyl-4-yl]methyl]piperidine (**16**·1.8H₂SO₄), isomer B. The compound was synthesized from **29f**. Yield: 55%; crystallized from Et₂O; mp: 92–98 °C (dec). ¹H NMR (DMSO-*d*₆, 300 MHz) δ 0.78 (t, *J* = 7.3 Hz, 3H), 1.02–0.85 (m, 1H), 1.40–1.04 (m, 6H), 1.80–1.40 (m, 5H), 2.18–1.90 (m, 4H), 3.07–2.65 (m, 3H), 3.70–3.10 (m, 7H), 4.20–3.90 (m, 2H), 4.50–4.20 (m, 1H), 7.57 (d, *J* = 8.1 Hz, 2H), 7.66 (d, *J* = 8.2 Hz, 2H), 7.80 (d, *J* = 8.0 Hz, 2H), 7.83 (d, *J* = 7.9 Hz, 2H), 9.48 (s, 1H). MS-(APCI): *m/z* 405.6 [M+1]⁺. Anal. Calcd for C₂₈H₄₀N₂·1.8H₂SO₄: C, 57.87; H, 7.56; N, 4.82. Found: C, 58.03; H, 7.73; N, 4.61.

6.1.10.9. (2*S*)-2-methyl-1-[[4'-(piperidin-1-ylmethyl)biphenyl-4-yl]pentyl]piperidine (**17**·1.95H₂SO₄), isomer A. The compound was synthesized from **29g**. Yield: 63%; crystallized from Et₂O; mp: 185–188 °C. ¹H NMR (CDCl₃, 300 MHz) δ 0.88 (t, *J* = 6.7 Hz, 3H), 1.20–1.08 (m, 2H), 1.22 (d, *J* = 6.1 Hz, 3H), 1.38–1.24 (m, 4H), 1.52–1.38 (m, 3H), 1.65–1.52 (m, 7H), 1.85 (q, *J* = 7.7 Hz, 2H), 1.98 (td, *J* = 10.8, 1.6 Hz, 2H), 2.28–2.15 (m, 1H), 2.50–2.30 (m, 4H), 2.97 (d, *J* = 11.3 Hz, 1H), 3.51 (s, 2H), 4.01 (t, *J* = 7.3 Hz, 1H), 7.28 (d, *J* = 8.0 Hz, 2H), 7.37 (d, *J* = 8.0 Hz, 2H), 7.54 (d, *J* = 7.9 Hz, 2H), 7.56 (d, *J* = 8.0 Hz, 2H). MS-(APCI): *m/z* 419.5 [M+1]⁺. Anal. Calcd for C₂₉H₄₂N₂·1.8H₂SO₄: C, 58.52; H, 7.72; N, 4.71. Found: C, 58.13; H, 7.74; N, 4.67.

6.1.10.10. (2*S*)-2-methyl-1-[[4'-(piperidin-1-ylmethyl)biphenyl-4-yl]pentyl]piperidine (**18**·1.8H₂SO₄), isomer B. The compound was synthesized from **29h**. Yield: 73%; crystallized from Et₂O; mp: 175–180 °C. ¹H NMR (CDCl₃, 300 MHz) δ 0.88 (t, *J* = 7.2 Hz, 3H), 1.22–1.15 (m, 2H), 1.15 (d, *J* = 6.3 Hz, 3H), 1.52–1.25 (m, 8H), 1.68–1.55 (m, 4H), 1.88–1.60 (m, 4H), 2.32–2.20 (m, 1H), 2.55–2.32 (m, 5H), 3.08–2.90 (m, 1H), 3.53 (s, 2H), 3.80 (dd, *J* = 9.8, 3.3 Hz, 1H), 7.38 (d, *J* = 7.9 Hz, 2H), 7.41 (d, *J* = 7.5 Hz, 2H), 7.55 (d, *J* = 7.9 Hz, 2H), 7.57 (d, *J* = 7.9 Hz, 2H). MS-(APCI): *m/z* 419.5 [M+1]⁺. Anal. Calcd for C₂₉H₄₂N₂·1.95H₂SO₄: C, 57.11; H, 7.59; N, 4.59. Found: C, 57.11; H, 7.62; N, 4.61.

6.1.10.11. 1-[[4'-(4-methoxy-1-((S)-2-methylpyrrolidin-1-yl)butyl)biphenyl-4-yl]methyl]piperidine (**19**·1.65H₂SO₄), isomer A. The compound was synthesized from **29i**. Yield: 60%; crystallized from Et₂O; mp: 98–102 °C (dec). ¹H NMR (CDCl₃, 300 MHz) δ 1.06 (d, *J* = 6.1 Hz, 3H), 1.55–1.23 (m, 10H), 1.75–1.55 (m, 2H), 1.95–1.75 (m, 2H), 2.38–2.25 (m, 5H), 2.40 (q, *J* = 6.2 Hz, 1H), 2.83 (ddd, *J* = 7.9, 7.2, 2.5 Hz, 1H), 3.19 (s, 3H), 3.26 (t, *J* = 6.6 Hz, 2H), 3.41 (s, 2H), 3.69 (dd, *J* = 8.8, 6.2 Hz, 1H), 7.17 (d, *J* = 8.1 Hz, 2H),

7.28 (d, $J = 8.2$ Hz, 2H), 7.43 (d, $J = 8.2$ Hz, 2H), 7.44 (d, $J = 8.2$ Hz, 2H). MS-(APCI): m/z 421.4 $[M+1]^+$. Anal. Calcd for $C_{28}H_{40}N_2O \cdot 1.65H_2SO_4$: C, 57.74; H, 7.49; N, 4.81. Found: C, 57.77; H, 7.72; N, 4.59.

6.1.10.12. 1-[[4'-(4-methoxy-1-((S)-2-methylpyrrolidin-1-yl)butyl)biphenyl-4-yl]methyl]piperidine (**20**·1.6H₂SO₄), isomer B. The compound was synthesized from **29j**. Yield: 67%. Crystallized from Et₂O; mp: 80–85 °C (dec). ¹H NMR (CDCl₃, 300 MHz) δ 0.78 (d, $J = 6.2$ Hz, 3H), 1.38–1.15 (m, 5H), 1.54–1.42 (m, 5H), 1.95–1.54 (m, 4H), 2.37–2.25 (m, 4H), 2.43 (q, $J = 8.9$ Hz, 1H), 2.75 (td, $J = 8.8, 4.1$ Hz, 1H), 2.95 (m, 1H), 3.17 (s, 3H), 3.21 (t, $J = 6.5$ Hz, 2H), 3.39 (dd, $J = 9.7, 3.8$ Hz, 1H), 3.40 (s, 2H), 7.26 (d, $J = 8.1$ Hz, 4H), 7.43 (d, $J = 8.3$ Hz, 2H), 7.44 (d, $J = 8.2$ Hz, 2H). MS-(APCI): m/z 421.4 $[M+1]^+$. Anal. Calcd for $C_{28}H_{40}N_2O \cdot 1.6H_2SO_4$: C, 58.23; H, 7.54; N, 4.85. Found: C, 58.23; H, 7.92; N, 4.62.

6.1.10.13. 1-[[4'-(1-((S)-2-methylpyrrolidin-1-yl)-4-phenoxybutyl)biphenyl-4-yl]methyl]piperidine (**21**·1.65H₂SO₄), isomer A. The compound was synthesized from **29k**. Yield: 86%; crystallized from Et₂O; mp: 110–115 °C (dec). ¹H NMR (CDCl₃, 300 MHz) δ 1.16 (d, $J = 6.0$ Hz, 3H), 1.90–1.25 (m, 12H), 2.20–1.95 (m, 2H), 2.50–2.35 (m, 6H), 2.93 (td, $J = 8.6, 3.0$ Hz, 1H), 3.51 (s, 2H), 3.85 (dd, $J = 8.4, 6.6$ Hz, 1H), 3.96 (t, $J = 6.5$ Hz, 2H), 6.87 (d, $J = 8.8$ Hz, 2H), 6.92 (t, $J = 7.7$ Hz, 1H), 7.26 (dd, $J = 8.5, 5.4$ Hz, 2H), 7.27 (d, $J = 8.9$ Hz, 2H), 7.38 (d, $J = 8.2$ Hz, 2H), 7.55 (d, $J = 8.2$ Hz, 2H), 7.56 (d, $J = 8.2$ Hz, 2H). MS-(APCI): m/z 483.2 $[M+1]^+$. Anal. Calcd for $C_{33}H_{42}N_2O \cdot 1.65H_2SO_4$: C, 61.49; H, 7.08; N, 4.35. Found: C, 61.48; H, 6.92; N, 4.13.

6.1.10.14. 1-[[4'-(1-((S)-2-methylpyrrolidin-1-yl)-4-phenoxybutyl)biphenyl-4-yl]methyl]piperidine (**22**·1.7H₂SO₄), isomer B. The compound was synthesized from **29l**. Yield: 75%; crystallized from Et₂O; mp: 140–145 °C (dec). ¹H NMR (CDCl₃, 300 MHz) δ 0.90 (d, $J = 5.9$ Hz, 3H), 1.52–1.28 (m, 4H), 1.85–1.56 (m, 7H), 2.08–1.85 (m, 2H), 2.25–2.17 (m, 1H), 2.50–2.30 (m, 4H), 2.60 (q, $J = 7.9$ Hz, 1H), 2.95–2.83 (m, 1H), 3.15–3.03 (m, 1H), 3.52 (s, 2H), 3.57 (dd, $J = 10.5, 3.7$ Hz, 1H), 3.89 (t, $J = 6.3$ Hz, 2H), 6.84 (d, $J = 8.6$ Hz, 2H), 6.92 (t, $J = 6.8$ Hz, 1H), 7.25 (t, $J = 7.8$ Hz, 2H), 7.38 (d, $J = 8.2$ Hz, 2H), 7.41 (d, $J = 8.4$ Hz, 2H), 7.56 (d, $J = 7.9$ Hz, 2H). MS-(APCI): m/z 483.4 $[M+1]^+$. Anal. Calcd for $C_{33}H_{42}N_2O \cdot 1.7H_2SO_4$: C, 61.03; H, 7.05; N, 4.31. Found: C, 60.98; H, 7.18; N, 4.04.

6.1.10.15. 1-[[4'-(4-(4-Methoxyphenoxy)-1-((S)-2-methylpyrrolidin-1-yl)-butyl)biphenyl-4-yl]methyl]piperidine (**23**·1.7H₂SO₄), isomer A. The compound was synthesized from **29m**. Yield: 62%; crystallized from Et₂O; mp: 153–161 °C (dec). ¹H NMR (CDCl₃, 300 MHz) δ 1.06 (d, $J = 6.0$ Hz, 3H), 1.40–1.26 (m, 3H), 1.53–1.40 (m, 5H), 1.75–1.58 (m, 4H), 2.10–1.85 (m, 2H), 2.41–2.27 (m, 6H), 2.83 (td, $J = 8.6, 3.0$ Hz, 1H), 3.42 (s, 2H), 3.66 (s, 3H), 3.74 (dd, $J = 8.3, 6.7$ Hz, 1H), 3.81 (t, $J = 6.5$ Hz, 2H), 6.72 (s, 4H), 7.18 (d, $J = 8.2$ Hz, 2H), 7.28 (d, $J = 8.2$ Hz, 2H), 7.45 (d, $J = 8.2$ Hz, 4H). MS-(APCI): m/z 513.3 $[M+1]^+$. Anal. Calcd for $C_{33}H_{44}N_2O_2 \cdot 1.7H_2SO_4$: C, 60.10; H, 7.03; N, 4.12. Found: C, 60.05; H, 7.10; N, 3.89.

6.1.10.16. 1-[[4'-(4-(4-Methoxyphenoxy)-1-((S)-2-methylpyrrolidin-1-yl)-butyl)biphenyl-4-yl]methyl]piperidine (**24**·2H₂SO₄), isomer B. The compound was synthesized from **29n**. Yield: 78%; crystallized from Et₂O; mp: 131–138 °C. ¹H NMR (CDCl₃, 300 MHz) δ 0.80 (d, $J = 6.3$ Hz, 3H), 1.40–1.26 (m, 3H), 1.72–1.40 (m, 8H), 1.90–1.74 (m, 2H), 2.10–1.98 (m, 1H), 2.37–2.25 (m, 4H), 2.44 (q, $J = 7.8$ Hz, 1H), 2.88 (ddd, $J = 8.9, 7.7, 4.1$ Hz, 1H), 2.96 (m, 1H), 3.42 (s, 2H), 3.44 (dd, $J = 10.6, 3.7$ Hz, 1H), 3.65 (s, 3H), 3.74 (t, $J = 6.4$ Hz, 2H), 6.70 (s, 4H), 7.28 (d, $J = 8.1$ Hz, 2H), 7.29 (d, $J = 8.2$ Hz, 2H), 7.45 (d,

$J = 8.3$ Hz, 2H), 7.46 (d, $J = 8.1$ Hz, 2H). MS-(APCI): m/z 513.3 $[M+1]^+$. Anal. Calcd for $C_{33}H_{44}N_2O_2 \cdot 2H_2SO_4$: C, 57.61; H, 6.83; N, 3.95. Found: C, 57.53; H, 6.73; N, 3.74.

6.1.10.17. 1-((4'-pentylbiphenyl-4-yl)methyl)piperidine (**34**·H₂SO₄). The compound was synthesized from **29o**. Yield: 90%; precipitated from Et₂O. ¹H NMR (CDCl₃, 300 MHz) δ 0.92 (t, $J = 6.8$ Hz, 3H), 1.34–1.39 (m, 4H), 1.46 (q, $J = 5.6$ Hz, 2H), 1.57–1.72 (m, 6H), 2.42 (m, 4H), 2.65 (t, $J = 7.5$ Hz, 2H), 3.52 (s, 2H), 7.25 (d, $J = 8.3$ Hz, 2H), 7.38 (d, $J = 8.3$ Hz, 2H), 7.52 (d, $J = 8.2$ Hz, 2H), 7.54 (d, $J = 8.2$ Hz, 2H). MS-(APCI): m/z 322.6 $[M+1]^+$. Anal. Calcd for $C_{23}H_{31}N \cdot H_2SO_4$: C, 65.84; H, 7.93; N, 3.34. Found: C, 65.60; H, 8.04; N, 3.11.

6.1.11. Preparation of (\pm)-1-(1-(4'-methylbiphenyl-4-yl)pentyl)piperidine (**35**·H₂SO₄)

The compound was synthesized via Suzuki coupling from **28p** and *p*-tolylboronic acid, following the procedure described for compounds **29a–n** and **31**. FC purification (CH₂Cl₂/CH₃OH(NH₃) 80:1) gave the desired product. Yield: 76%; crystallized from Et₂O; mp: 120–122 °C. NMR (CDCl₃, 300 MHz) δ 0.86 (t, $J = 7.0$ Hz, 3H), 1.10–1.18 (m, 2H), 1.28–1.39 (m, 4H), 1.53–1.63 (m, 4H), 1.82–1.95 (m, 2H), 2.39 (m, 4H), 2.41 (s, 3H), 3.37 (dd, $J = 9.2, 5.1$ Hz, 1H), 7.26 (d, $J = 7.9$ Hz, 2H), 7.27 (d, $J = 8.1$ Hz, 2H), 7.53 (d, $J = 8.0$ Hz, 2H), 7.55 (d, $J = 8.2$ Hz, 2H). MS-(APCI): m/z 322.4 $[M+1]^+$. Anal. Calcd for $C_{23}H_{31}N \cdot H_2SO_4$: C, 65.84; H, 7.93; N, 3.34. Found: C, 65.84; H, 7.92; N, 3.33.

6.2. Pharmacology

Drugs used were purchased from Sigma (St. Louis, MA, USA). Cultured SK-N-MC cells stably expressing human histamine H₃ receptors and the reporter gene β -galactosidase (Johnson & Johnson Pharmaceutical Research and Development, L.L.C.) were used for binding and functional studies. Functional experiments were also performed on isolated ileal and atrial tissues excised from guinea-pigs (250–350 g). Animals were housed, handled and cared for according to the European Community Council Directive 86 (609) EEC and the experimental protocols were carried out in compliance with Italian regulations (DL 116/92) and with the local Ethical Committee Guidelines for Animal Research.

6.2.1. Human histamine H₃ and H₄ receptor binding assay

Homogenates of SK-N-MC cells, a human neuroblastoma cell line stably expressing the human histamine H₃ and H₄ receptors, were used in radioligand displacement studies according to literature methods [38,49]. Membranes were incubated for 60 min at room temperature with 0.5 nM [³H]-(R)- α -methylhistamine (47.0 Ci/mmol, Amersham Bioscience) or with 10 nM [³H]-histamine (18.1 Ci/mmol, Perkin Elmer) in the absence or in the presence of competing ligands (0.01 nM–10 μ M). Incubation was terminated by rapid filtration over Millipore AAWPO2500 filters followed by two washes with ice-cold buffer (50 mM Tris–HCl/5 mM EDTA). Nonspecific binding was defined by 10 μ M histamine as competing ligand.

6.2.2. Rat histamine H₃ receptor binding assay

Rat brain membranes, prepared according to Kilpatrick's method [50], were incubated for 45 min with [³H]-(R)- α -methylhistamine 0.5 nM and the compounds under study (0.03 nM–10 μ M), in Tris–HCl 50 mM, pH 7.4, NaCl 50 mM, EDTA 0.5 mM, then rapidly filtered (AAWP Millipore filters 0.8 μ m) under vacuum and rinsed twice with the same ice-cold buffer. Nonspecific binding was defined by 10 μ M thioperamide as competing ligand.

6.2.3. Human histamine H₃ receptor functional assay

Compounds were added directly to the media containing SK-N-MC cells expressing the human histamine H₃ receptor as well as the

construct gene (β -galactosidase), followed, 5 min later, by addition of forskolin (5 μ M). The compounds (1 nM–10 μ M) were added 10 min prior to (*R*)- α -methylhistamine (0.1–100 nM). After a 6 h incubation at 37 °C, the medium was aspirated and the cells were lysed with 25 μ L of 1 \times assay buffer (mM composition: NaH₂PO₄ 10, Na₂HPO₄ 10, pH 8, MgSO₄ 0.2, MnCl₂ 0.01) and after 10 min with 100 μ L of 1 \times assay buffer (NaH₂PO₄ 100, Na₂HPO₄ 100, pH 8, MgSO₄ 2, MnCl₂ 0.1) containing 0.5% Triton and 40 mM β -mercaptoethanol. Color was developed using 25 μ L of 1 mg/mL substrate solution (chlorophenol red β -D-galactopyranoside; Roche Molecular Biochemicals, Indianapolis, IN, USA) and quantitated on a microplate reader by measuring the absorbance at 570 nm (Biorad microplate reader 550, Segrate, MI, Italy) [40].

6.2.4. Guinea-pig histamine H₁ and H₂ receptor functional assay

Portions of guinea-pig ileum were longitudinally mounted (1 g load) in organ chambers, filled with Krebs–Henseleit solution (mM composition: NaCl 118.9, KCl 4.6, CaCl₂ 2.5, KH₂PO₄ 1.2, NaHCO₃ 25, MgSO₄ 1.2, glucose 11.1) and gassed with 95% O₂–5% CO₂ at 37 °C. Spontaneously beating isolated atria were isometrically mounted (0.5 g load) in organ chambers filled with Ringer–Locke solution (mM composition: NaCl 154.0, KCl 5.6, CaCl₂ 1.08, NaHCO₃ 5.95, glucose 11.1). Atrial responses were determined as changes in the rate of spontaneous beating by means of a connected cardiograph. Cumulative dose–response curves of histamine in the ileum (1 nM–1 μ M) or of the H₂-agonist dimaprit in the atria (0.1–100 μ M) were obtained in the absence and presence of the compounds tested, up to a concentration of 10 μ M, to ascertain their H₁ and H₂ antagonistic activity [41].

6.2.5. Data analysis

The data are presented as means \pm SEM. In functional tests results are expressed as percentage of the maximum response induced by the agonist. The antagonistic affinities were estimated determining pK_B as described by Furchgott's equation [51]. When non-surmountable antagonism was detected, the antagonistic potency of the drugs was expressed by pD₂' values determined according to Van Rossum's equation [52].

In binding assays, pIC₅₀ values were estimated from the displacement curves of the tested compounds versus [³H]- α -methylhistamine or [³H]-histamine and converted to pK_i values according to Cheng and Prusoff's equation [53].

6.2.6. Human muscle-type nicotinic receptor binding assay

The test was performed by Cerep [54]. Cell membrane homogenates (60 μ g protein) were incubated for 120 min at 22 °C with 0.5 nM [¹²⁵I]- α -bungarotoxin in the absence or presence of the test compound in a buffer containing 20 mM Hepes/NaOH (pH 7.3), 118 mM NaCl, 4.8 mM KCl, 2.5 mM CaCl₂, 1.2 mM MgSO₄ and 0.1% BSA [55]. Nonspecific binding was determined in the presence of 5 μ M α -bungarotoxin. Following incubation, the samples were filtered rapidly under vacuum through glass fiber filters (GF/B, Packard) presoaked with 0.3% PEI and rinsed several times with an ice-cold buffer containing 50 mM Tris–HCl, 150 mM NaCl and 0.1% BSA using a 96-sample cell harvester (Unifilter, Packard). The filters were dried then counted for radioactivity in a scintillation counter (Topcount, Packard) using a scintillation cocktail (Microscint 0, Packard). The results are expressed as a percent inhibition of the control radioligand (α -bungarotoxin) specific binding. The percent inhibition of [¹²⁵I]- α -bungarotoxin binding exerted by compound **21** was evaluated at 100 and 1 μ M, in experiments performed in duplicate.

6.2.7. Human α 7 neuronal nicotinic receptor binding assay

The test was performed by Cerep [54]. Cell membrane homogenates (20 μ g protein) were incubated for 120 min at 37 °C with

0.05 nM [¹²⁵I]- α -bungarotoxin in the absence or presence of the test compound in a buffer containing 50 mM K₂HPO₄/KH₂PO₄ (pH 7.4), 10 mM MgCl₂ and 0.1% BSA [56]. Nonspecific binding was determined in the presence of 1 μ M α -bungarotoxin. Following incubation, the samples were filtered rapidly under vacuum through glass fiber filters (GF/B, Packard) presoaked with 0.3% PEI and rinsed several times with ice-cold 50 mM Tris–HCl using a 96-sample cell harvester (Unifilter, Packard). The filters were dried then counted for radioactivity in a scintillation counter (Topcount, Packard) using a scintillation cocktail (Microscint 0, Packard). The results are expressed as a percent inhibition of the control radioligand (α -bungarotoxin) specific binding. The percent inhibition of [¹²⁵I]- α -bungarotoxin binding exerted by compound **21** was evaluated at 100 and 1 μ M, in experiments performed in duplicate.

6.3. Molecular modeling

6.3.1. Molecular dynamics simulations

Molecular modeling studies were performed with MacroModel 9.8 [57]. Starting structures of (*S,R*) and (*R,R*) isomers of {4'-[1-(2-methylpyrrolidin-1-yl)pentyl]biphenyl-4-yl}methanol (**29c,d**) were optimized with the MM3 force field [58], using a convergence criterion of 0.05 kJ mol⁻¹ Å⁻¹. Stochastic dynamics (SD) simulations were performed employing the MM3 force field, applying the GB/SA [59] CHCl₃ solvation treatment. SD was conducted for 1 μ s to a temperature of 298 K, after 1000 ps of equilibration, applying a time step of 1 fs. 10,000 snapshots were collected for data analysis. SD has already proved to be able to reproduce the conformational equilibrium of small molecules in CHCl₃ applying an implicit treatment of solvent molecules [60–66]. Proton–proton coupling constants were calculated with the software Maestro 9.1 [67], employing an implemented version of the Karplus equation [68].

6.3.2. H₃ receptor homology modeling and docking

The X-ray crystal structure of the histamine H₁ receptor (PDB ID: 3RZE) [44] was used as template for the H₃ receptor modeling. The amino acid sequence of the human H₃ receptor was retrieved from the Universal Protein Resource (UniProt ID: Q9Y5N1) [69,70]. Initial alignment was carried out with ClustalW2 [71] using default parameters and subsequently optimized considering conserved sequence motifs among class A GPCRs [72–74]. Highly conserved residues within transmembrane (TM) domains [72], as well as the conserved disulfide bridge connecting the extracellular loop (ECL) 2 and TM3 have been taken into account during alignment refinement. The disulfide bond connecting ECL3 and the top of TM6 in the H₁ histamine receptor crystal structure was also considered during the optimization of the sequence alignment (Figure S6). Since T4-lysozyme replaced intracellular loop 3 (ICL3) in the H₁ receptor crystal structure, the corresponding sequence of the H₃ receptor was excluded from homology modeling procedure and Thr229 at the end of TM5 was linked to Phe348 belonging to the last portion of ICL3. This should not impact the ligand docking experiments, since the binding pocket of H₃ receptor is located near the extracellular region.

Comparative modeling was carried out with Modeller 9v7 [75] and thirty H₃ receptor models were initially generated. The stereochemical quality of the models was evaluated using Procheck [76], as well as the Protein Report tool implemented in Maestro 9.1. The best model was selected on the basis of geometrical parameters quality and on Modeller objective function. Since the ECL2 portion is known to play an important role in shaping the binding site and could be directly involved in ligand stabilization, the selected receptor model was submitted to an additional refinement procedure, in which the terminal segment of ECL2 (from Tyr189 to Asn195) was optimized using Modeller 9v7. The final H₃ receptor model was then refined with the Protein Preparation Wizard

workflow of Maestro 9.1. Hydrogen atoms were added and protonation states for ionizable side chains were chosen to be consistent with physiological pH and to allow the widest possible networks of hydrogen-bonds. Chain termini were capped with neutral groups (acetyl and methylamino) and the all-hydrogen receptor model was subjected to restrained molecular mechanics refinement to a RMSD of 0.3 Å with the OPLS2005 force field [77]. The Ramachandran plot for the final refined structure is reported in Figure S7.

Compounds **6–24** were built with Maestro 9.1 and energy-minimized using the OPLS2005 force field to a convergence threshold of 0.05 kJ/(mol/Å). All isomers were considered for those compounds being tested as mixtures of enantiomers or diastereoisomers. An induced-fit docking (IFD) [78,79] was applied to account for receptor flexibility during docking simulations. During the initial softened-potential docking, the ligands were docked into a rigid receptor model with scaled-down van der Waals (vdW) radii: a vdW scaling of 0.5 was used for both protein and ligand non-polar atoms. Leu76, Asp80, Val83, Ser121, Met378, Trp402 and Asn408 were temporarily mutated to alanines, to enlarge the binding site. Asp114 was used to define the location of the binding site and the dimension of the energy grids during the initial softened-potential docking. Initial docking runs were performed applying a hydrogen-bond constraint to Asp114: a hydrogen-bond constraint was applied between Asp114 and the protonated nitrogen bound to the chiral benzylic carbon. No constraint was used for compounds **6–8**. Docking runs were performed using standard precision (SP) mode and retaining twenty ligand poses for subsequent protein structural refinement. Each complex was then subjected to side chain and backbone refinements using Prime. Side chains previously removed were re-introduced and all residues with at least one atom located within 6.0 Å from the ligand were included in the Prime refinement stage. The conserved tryptophan residue of the CWXP motif (Trp371) was kept fixed during Prime refinement, since no significant conformational changes are expected after antagonist binding. Finally, each ligand pose was re-docked into its refined low-energy receptor structure, using default Glide settings (vdW radii scaling of 1.0 for receptor and 0.8 for the ligand non-polar atoms) and re-applying the hydrogen-bond constraint to Asp114. The final ligand–protein complexes were ranked according to their IFD score. The IFD score is a composite score that accounts for ligand–receptor interaction energy (GlideScore), receptor strain and solvation terms (Prime Energy) [79]. It is calculated as follows: IFD score (Kcal/mol) = GlideScore + 0.05 × Prime Energy.

Reference compound **6** was initially docked to evaluate its binding orientations into the new H₃ receptor model. Two different binding modes were obtained, corresponding to the “horizontal” and the “vertical” ones previously observed [26] (see Introduction for description). Receptor–ligand complexes for **23** and **24** having the best IFD score were energy-minimized with the OPLS2005 force field to a convergence threshold of 0.1 kJ/(mol/Å). The final complexes are depicted in Fig. 7.

Acknowledgment

The C.I.M. (Centro Interdipartimentale Misura) of the University of Parma is gratefully acknowledged for providing NMR instrumentation. The authors wish to thank Dr. Domenico Acquotti for skillful technical assistance.

Appendix. Supplementary data

Supplementary data associated with this article can be found, in the online version, at doi:10.1016/j.ejmech.2011.12.019

References

- [1] L.B. Hough, Genomics meets histamine receptors: new subtypes, new receptors, *Mol. Pharmacol.* 59 (2001) 415–419.
- [2] R. Leurs, M.K. Chirch, M. Tagliatela, H₁-antihistamines: inverse agonism, anti-inflammatory actions and cardiac effects, *Clin. Exp. Allergy* 32 (2002) 489–498.
- [3] W. Schunack, Pharmacology of H₂-receptor antagonists: an overview, *J. Int. Med. Res.* 17 (1989) 9A–16A.
- [4] M. Zhang, R.L. Thurmod, P. Dunford, The histamine H₄ receptor: a novel modulator of inflammatory and immune disorders, *Pharmacol. Ther.* 113 (2007) 594–606.
- [5] J.-M. Arrang, M. Garbarg, J.-C. Schwartz, Auto-inhibition of brain histamine release mediated by a novel class (H₃) of histamine receptor, *Nature* 302 (1983) 832–837.
- [6] J. Gomez-Ramirez, J. Ortiz, I. Blanco, Presynaptic H₃ autoreceptors modulate histamine synthesis through cAMP pathway, *Mol. Pharmacol.* 61 (2002) 239–245.
- [7] E. Schlicker, K. Fink, M. Hinterthaler, M. Gothert, Inhibition of noradrenaline release in the rat brain cortex via presynaptic H₃ receptors, *Naunyn-Schmiedeberg's Arch. Pharmacol.* 340 (1989) 633–638.
- [8] C. Blandizzi, M. Toghetti, R. Colucci, M. Del Tacca, Histamine H₃ receptors mediate inhibition of noradrenaline release from intestinal sympathetic nerves, *Br. J. Pharmacol.* 129 (2000) 1387–1396.
- [9] E. Schlicker, K. Fink, M. Detzner, M. Gothert, Histamine inhibits dopamine release in the mouse striatum via presynaptic H₃ receptors, *J. Neural Transm. Gen. Sect.* 93 (1993) 1–10.
- [10] E. Schlicker, R. Berz, M. Gothert, Histamine H₃ receptor-mediated inhibition of serotonin release in the rat brain cortex, *Naunyn-Schmiedeberg's Arch. Pharmacol.* 337 (1988) 588–590.
- [11] F. Bergquist, A. Ruthven, M. Ludwig, M.B. Dutia, Histaminergic and glycinergic modulation of GABA release in the vestibular nuclei of normal and labyrinthectomised rats, *J. Physiol.* 577 (2006) 857–868.
- [12] B. Garduño-Torres, M. Treviño, R. Gutierrez, J.A. Arias-Montañón, Pre-synaptic histamine H₃ receptors regulate glutamate, but not GABA release in rat thalamus, *Neuropharmacology* 52 (2007) 527–535.
- [13] P. Blandina, M. Giorgetti, L. Bartolini, M. Cecchi, H. Timmerman, R. Leurs, G. Pepeu, M.G. Giovannini, Inhibition of cortical acetylcholine release and cognitive performance by histamine H₃ receptor activation in rats, *Br. J. Pharmacol.* 119 (1996) 1656–1664.
- [14] A.A. Hancock, G.B. Fox, Drugs that target histaminergic receptors, in: J.J. Buccafusco (Ed.), *Cognition Enhancing Drugs*, Birkhäuser Verlag, Basel Switzerland, 2004, pp. 97–114.
- [15] M.A.M.R. De Almeida, I. Izquierdo, Intracerebroventricular histamine, but not 48/80, causes posttraining memory facilitation in the rat, *Arch. Int. Pharmacodyn. Ther.* 291 (1988) 202–207.
- [16] R. Leurs, R.A. Bakker, H. Timmerman, I.J.P. de Esch, The histamine H₃ receptor: from gene cloning to H₃ receptor drugs, *Nat. Rev. Drug Discov.* 4 (2005) 107–120.
- [17] K. Sander, T. Kottke, H. Stark, Histamine H₃ receptor antagonists go to clinics, *Biol. Pharm. Bull.* 31 (2008) 2163–2181.
- [18] M.J. Gemkow, A.J. Davenport, S. Harich, B.A. Ellenbroek, The histamine H₃ receptor as a therapeutic drug target for CNS disorders, *Drug Discov. Today* 14 (2009) 509–515.
- [19] D. Lazewska, K. Kiec-Kononowicz, Recent advances in histamine H₃ receptor antagonists/inverse agonists, *Expert Opin. Ther. Patents* 20 (2010) 1147–1169.
- [20] M. Berlin, C.W. Boyce, M. de Lera Ruiz, Histamine H₃ receptor as a drug discovery target, *J. Med. Chem.* 54 (2011) 26–53.
- [21] D. Yokoyama Vohora, Histamine-selective H₃ receptor ligands and cognitive functions: an overview, *IDrugs* 7 (2004) 667–673.
- [22] H. Stark, J.-M. Arrang, X. Ligneau, M. Garbarg, C.R. Ganellin, J.-C. Schwartz, W. Schunack, The histamine H₃ receptor and its ligands, *Prog. Med. Chem.* 38 (2001) 279–308.
- [23] M. Cowart, R. Altenbach, L. Black, R. Faghieh, C. Zhao, A.A. Hancock, Medicinal chemistry and biological properties of non-imidazole histamine H₃ antagonists, *Mini-Rev. Med. Chem.* 4 (2004) 979–992.
- [24] S. Celanire, M. Wijtmans, P. Talaga, R. Leurs, I.J.P. de Esch, Keynote review: histamine H₃ receptor antagonists reach out for the clinic, *Drug Discov. Today* 10 (2005) 1613–1627.
- [25] E.P. Lebois, C.K. Jones, C.W. Lindsley, The evolution of histamine H₃ antagonists/inverse agonists, *Curr. Top. Med. Chem.* 11 (2011) 648–660.
- [26] G. Morini, M. Comini, M. Rivara, S. Rivara, S. Lorenzi, F. Bordi, M. Mor, L. Flammini, S. Bertoni, V. Ballabeni, E. Barocelli, P.V. Plazzi, Dibasic non-imidazole histamine H₃ receptor antagonists with a rigid biphenyl scaffold, *Bioorg. Med. Chem. Lett.* 16 (2006) 4063–4067.
- [27] G. Morini, M. Comini, M. Rivara, S. Rivara, F. Bordi, P.V. Plazzi, L. Flammini, F. Sacconi, S. Bertoni, V. Ballabeni, E. Barocelli, M. Mor, Synthesis and structure-activity relationships for biphenyl H₃ receptor antagonists with moderate anticholinesterase activity, *Bioorg. Med. Chem.* 16 (2008) 9911–9924.
- [28] M. Rivara, V. Zuliani, G. Coconcelli, G. Morini, M. Comini, S. Rivara, M. Mor, F. Bordi, E. Barocelli, V. Ballabeni, S. Bertoni, P.V. Plazzi, Synthesis and biological evaluation of new non-imidazole H₃-receptor antagonists of the 2-aminobenzimidazole series, *Bioorg. Med. Chem.* 14 (2006) 1413–1424.
- [29] E. Barocelli, V. Ballabeni, V. Manenti, L. Flammini, S. Bertoni, G. Morini, M. Comini, M. Impicciatore, Discovery of histamine H₃ receptor antagonistic property of simple imidazole-free derivatives: preliminary pharmacological investigation, *Pharmacol. Res.* 53 (2006) 226–232.

- [30] B.B. Yao, C.W. Hutchins, T.L. Carr, S. Cassar, J.N. Masters, Y.L. Bennani, T.A. Esbenshade, A.A. Hancock, Molecular modeling and pharmacological analysis of species-related histamine H₃ receptor heterogeneity, *Neuropharmacology* 44 (2003) 773–786.
- [31] F.U. Axe, S.D. Bembenek, S. Szalma, Three-dimensional models of histamine H₃ receptor antagonist complexes and their pharmacophore, *J. Mol. Graph. Model.* 24 (2006) 456–464.
- [32] B. Schlegel, C. Lagner, R. Meier, T. Langer, D. Schnell, R. Seifert, H. Stark, H.-D. Holtje, W. Sippl, Generation of a homology model of the human histamine H₃ receptor for ligand docking and pharmacophore-based screening, *J. Comput. Aided Mol. Des.* 21 (2007) 437–453.
- [33] N. Levoine, T. Calmels, O. Poupardin-Oliveier, O. Labeeuw, D. Danvy, P. Robert, I. Berrebi-Bertrand, C.R. Ganellin, W. Schunack, H. Stark, M. Capet, Refined docking as a valuable tool for lead optimization: application to histamine H₃ receptor antagonists, *Arch. Pharm. Chem. Life Sci.* 341 (2008) 610–623.
- [34] B.K. Rai, G.J. Tawa, A.H. Katz, C. Humblet, Modeling G protein-coupled receptors for structure-based drug discovery using low-frequency normal modes for refinement of homology models: application to H₃ antagonists, *Proteins* 78 (2010) 457–473.
- [35] O. Roche, R.M. Rodriguez Sarmiento, A new class of histamine H₃ receptor antagonists derived from ligand based design, *Bioorg. Med. Chem. Lett.* 17 (2007) 3670–3675.
- [36] K.S. Ly, M.A. Letavic, J.M. Keith, J.M. Miller, E.M. Stocking, A.J. Barbier, P. Bonaventure, B. Lord, X. Jiang, J.D. Boggs, L. Dvorak, K.L. Miller, D. Nepomuceno, S.J. Wilson, N.I. Carruthers, Synthesis and biological activity of piperazine and diazepane amides that are histamine H₃ antagonists and serotonin reuptake inhibitors, *Bioorg. Med. Chem. Lett.* 18 (2008) 39–43.
- [37] M.A. Letavic, J.M. Keith, J.A. Jablonowski, E.M. Stocking, L.A. Gomez, K.S. Ly, J.M. Miller, A.J. Barbier, P. Bonaventure, J.D. Boggs, S.J. Wilson, K.L. Miller, B. Lord, H.M. McAllister, D.J. Tognarelli, J. Wu, M.C. Abad, C. Schubert, T.W. Lovenberg, N.I. Carruthers, Novel tetrahydroisoquinolines are histamine H₃ antagonists and serotonin reuptake inhibitors, *Bioorg. Med. Chem. Lett.* 17 (2007) 1047–1051.
- [38] T.W. Lovenberg, B.L. Roland, S.J. Wilson, X. Jiang, J. Pyati, A. Huvar, M.R. Jackson, M.G. Erlander, Cloning and functional expression of the human histamine H₃ receptor, *Mol. Pharmacol.* 55 (1999) 1101–1107.
- [39] P.V. Plazzi, F. Bordi, M. Mor, C. Silva, G. Morini, A. Caretta, E. Barocelli, T. Vitali, Heteroaryl aminoethyl and eteroarythioethyl imidazoles. Synthesis and H₃-receptor affinity, *Eur. J. Med. Chem.* 30 (1995) 881–889.
- [40] R. Apodaca, C.A. Dvorak, W. Xiao, A.J. Barbier, J.D. Boggs, S.J. Wilson, T.W. Lovenberg, N.I. Carruthers, A new class of diamine-based human histamine H₃ receptor antagonists: 4-(aminoalkoxy)benzylamines, *J. Med. Chem.* 46 (2003) 3938–3944.
- [41] S. Bertoni, V. Ballabeni, L. Flammini, F. Saccani, G. Domenichini, G. Morini, M. Comini, M. Rivara, E. Barocelli, In vitro and in vivo pharmacological analysis of imidazole-free histamine H₃ receptor antagonists: promising results for a brain-penetrating H₃ blocker with weak anticholinesterase activity, *Naunyn Schmiedeberg's Arch. Pharmacol.* 378 (2008) 335–343.
- [42] D.L. Nersesian, L.A. Black, T.R. Miller, T.A. Vortherms, T.A. Esbenshade, A.A. Hancock, M.D. Cowart, In vitro SAR of pyrrolidine-containing histamine H₃ receptor antagonists: trends across multiple chemical series, *Bioorg. Med. Chem. Lett.* 18 (2008) 355–359.
- [43] M. Cowart, R. Faghiih, M.P. Curtis, G.A. Gfesser, Y.L. Bennani, L.A. Black, L. Pan, K.C. Marsh, J.P. Sullivan, T.A. Esbenshade, G.B. Fox, A.A. Hancock, 4-(2-[2-(2(R)-methylpyrrolidin-1-yl)ethyl]benzofuran-5-yl)benzotrile and related 2-aminoethylbenzofuran H₃ receptor antagonists potently enhance cognition and attention, *J. Med. Chem.* 48 (2005) 38–55.
- [44] T. Shimamura, M. Shiroishi, S. Weyand, H. Tsujimoto, G. Winter, V. Katritch, R. Abagyan, V. Cherezov, W. Liu, G.W. Han, T. Kobayashi, R.C. Stevens, S. Iwata, Structure of the human histamine H₁ receptor complex with doxepin, *Nature* 475 (2011) 65–70.
- [45] S. Lorenzi, M. Mor, F. Bordi, S. Rivara, M. Rivara, G. Morini, S. Bertoni, V. Ballabeni, E. Barocelli, P.V. Plazzi, Validation of a histamine H₃ receptor model through structure-activity relationships for classical H₃ antagonists, *Bioorg. Med. Chem.* 19 (2005) 5647–5657.
- [46] (a) R. Leurs, M.J. Smit, C.P. Tensen, A.M. Terlaak, H. Timmerman, Site-directed mutagenesis of the histamine H₁-receptor reveals a selective interaction of asparagine207 with subclasses of H₁-receptor agonists, *Biochem. Biophys. Res. Commun.* 201 (1994) 295–301; (b) N. Moguilevsky, F. Varsalona, J.P. Guillaume, M. Noyer, M. Gillard, J. Daliers, J.P. Henichart, A. Bollen, Pharmacological and functional characterisation of the wild-type and site-directed mutants of the human H₁ histamine receptor stably expressed in CHO cells, *J. Recept. Signal. Transduct. Res.* 15 (1995) 91–102.
- [47] A.J. Uveges, D. Kowal, Y. Zhang, T.B. Spangler, J. Dunlop, S. Semus, P.G. Jones, The role of transmembrane Helix5 in agonist binding to the human H₃ receptor, *J. Pharmacol. Exp. Ther.* 301 (2002) 451–458.
- [48] P.A. Gemmill, G.W. Gray, D. Lacey, A.K. Alimoglu, A. Ledwith, Polymers with rigid anisotropic side groups. 2. Synthesis and properties of some side chain acrylate and methacrylate liquid crystal polymers containing the 4'-alkylbi-phenyl-4-yl moiety, *Polymer* 26 (1985) 615–621.
- [49] C. Liu, X. Ma, X. Jiang, S.J. Wilson, C.L. Hofstra, J. Blevitt, J. Pyati, X. Li, W. Chai, N. Carruthers, T.W. Lovenberg, Cloning and pharmacological characterization of a fourth histamine receptor (H₄) expressed in bone marrow, *Mol. Pharmacol.* 59 (2001) 420–426.
- [50] G.J. Kilpatrick, A.D. Michel, Characterisation of the binding of the histamine H₃ receptor agonist [3H] (R)-alpha methyl histamine to homogenates of rat and guinea-pig cortex, *Agents Actions Suppl.* 33 (1991) 69–75.
- [51] R.F. Furchgott, in: E. Blanschko, E. Muscholl (Eds.), *Handbook of Experimental Pharmacology*, vol. 33, Springer, Berlin, 1972, pp. 283–335.
- [52] J.M. Van Rossum, Cumulative dose-response curves. II. Technique for the making of dose-response curves in isolated organs and the evaluation of drug parameters, *Arch. Int. Pharmacodyn. Ther.* 143 (1963) 299–330.
- [53] Y. Cheng, W.H. Prusoff, Relationship between the inhibition constant (K_i) and the concentration of inhibitor which causes 50 per cent inhibition (I₅₀) of an enzymatic reaction, *Biochem. Pharmacol.* 22 (1973) 3099–3108.
- [54] www.cerep.com.
- [55] R.J. Lukas, Characterization of curaremimetic neurotoxin binding sites on membrane fractions derived from the human medulloblastoma clonal line, TE671, *J. Neurochem.* 46 (1986) 1936–1941.
- [56] C.G.V. Sharples, S. Kaiser, L. Soliakov, M.J. Marks, A.C. Collins, M. Washburn, E. Wright, J.A. Spencer, T. Gallagher, P. Whiteaker, P. S. Wonnacott, UB-165: a novel nicotinic agonist with subtype selectivity implicates the a4b2 subtype in the modulation of dopamine release from rat striatal synaptosomes, *J. Neurosci.* 20 (2000) 2783–2791.
- [57] MacroModel, Version 9.8, Schrödinger, LLC, New York, NY, 2010.
- [58] N.L. Allinger, Y.H. Yuh, J.-H. Lii, Molecular mechanics. The MM3 force field for hydrocarbons. 1, *J. Am. Chem. Soc.* 111 (1989) 8551–8566.
- [59] W.C. Still, A. Tempczyk, R.C. Hawley, T. Hendrickson, Semianalytical treatment of solvation for molecular mechanics and dynamics, *J. Am. Chem. Soc.* 112 (1990) 6127–6129.
- [60] R.M. Brunne, W.F. van Gusteren, R. Brueschweiler, R.R. Ernst, Molecular dynamics simulation of the proline conformational equilibrium and dynamics in antamanide using the GROMOS force field, *J. Am. Chem. Soc.* 115 (1993) 4764–4768.
- [61] L.A. Christianson, M.J. Lucero, D.H. Appella, D.A. Klein, S.H. Gellman, Improved treatment of cyclic β-amino acids and successful prediction of β-peptide secondary structure using a modified force field: aMBER**C*, *J. Comput. Chem.* 21 (2000) 763–773.
- [62] C. Dolain, J.-M. Léger, N. Delsuc, H. Gornitzka, I. Huc, Probing helix propensity of monomers within a helical oligomer, *Proc. Natl. Acad. Sci. USA* 102 (2005) 16146–16151.
- [63] D.Q. McDonald, W.C. Still, An AMBER* study of Gellman's amides, *Tetrahedron Lett.* 33 (1992) 7747–7750.
- [64] C. Palocci, M. Falconi, S. Alcaro, A. Tafi, R. Puglisi, F. Ortuso, M. Botta, L. Alberghina, E. Cernia, An approach to address *Candida rugosa* lipase regioselectivity in the acylation reactions of tritylated glucosides, *J. Biotechnol.* 128 (2007) 908–918.
- [65] V. Berl, I. Huc, R.G. Khoury, J.-M. Lehn, Helical molecular programming: folding of oligopyridine-dicarboxamides into molecular single helices, *Chem. Eur. J.* 7 (2001) 2798–2809.
- [66] V. Berl, I. Huc, R.G. Khoury, J.-M. Lehn, Helical molecular programming: supramolecular double helices by dimerization of helical oligopyridine-dicarboxamide strands, *Chem. Eur. J.* 7 (2001) 2810–2820.
- [67] Maestro, Version 9.1, Schrödinger, LLC, New York, NY, 2010.
- [68] C.A.G. Haasnoot, F.A.A.M. de Leeuw, C. Altona, The relationship between proton-proton NMR coupling constants and substituent electronegativity –I: an empirical generalization of the Karplus equation, *Tetrahedron* 36 (1979) 2783–2792.
- [69] The UniProt Consortium, Ongoing and future developments at the universal protein resource, *Nucleic Acids Res.* 39 (2011) D214–D219.
- [70] E. Jain, A. Bairoch, S. Duvaud, I. Phan, N. Redaschi, B.E. Suzek, M.J. Martin, P. McGarvey, E. Gasteiger, Infrastructure for the life sciences: design and implementation of the UniProt website, *BMC Bioinform.* 10 (2009) 136.
- [71] J.D. Thompson, D.G. Higgins, T.J. Gibson, CLUSTAL W: improving the sensitivity of progressive multiple sequence alignment through sequence weighting, position-specific gap penalties and weight matrix choice, *Nucleic Acids Res.* 22 (1994) 4673–4680.
- [72] J.A. Ballesteros, H. Weinstein, Integrated methods for the construction of three-dimensional models and computational probing of structure-function relations in G protein-coupled receptors, in: S.C. Sealfon, P.M. Conn (Eds.), *Methods in Neurosciences*, 25, Academic Press, San Diego (CA), 1995, pp. 366–428.
- [73] J.A. Ballesteros, L. Shi, J.A. Javitch, Structural mimicry in G protein-coupled receptors: implications of the high-resolution structure of rhodopsin for structure-function analysis of rhodopsin-like receptors, *Mol. Pharmacol.* 60 (2001) 1–19.
- [74] A. Rayan, New vistas in GPCR 3D structure prediction, *J. Mol. Model.* 16 (2010) 183–191.
- [75] A. Sali, T.L. Blundell, Comparative protein modelling by satisfaction of spatial restraints, *J. Mol. Biol.* 234 (1993) 779–815.
- [76] R.A. Laskowski, M.W. MacArthur, D.S. Moss, J.M. Thornton, PROCHECK: a program to check the stereochemical quality of protein structures, *J. Appl. Cryst.* 26 (1993) 283–291.
- [77] G.A. Kaminski, R.A. Friesner, J. Tirado-Rives, W.L. Jorgensen, Evaluation and reparameterization of the OPLS-AA force field for proteins via comparison with accurate quantum chemical calculations on peptides, *J. Phys. Chem. B.* 105 (2001) 6474–6487.
- [78] W. Sherman, T. Day, M.P. Jacobson, R.A. Friesner, R. Farid, Novel procedure for modeling ligand/receptor induced fit effects, *J. Med. Chem.* 49 (2006) 534–553.
- [79] Schrödinger Suite 2010 Induced Fit Docking Protocol; Glide Version 5.6, Schrödinger, LLC, New York, NY, 2010, Prime version 2.2, Schrödinger, LLC, New York, NY, 2010.